# Dynamical Phenomena including Many Body Effects at Metal Surfaces

Hideaki Kasai* and Wilson Agerico Diño†
*Department of Applied Physics, Osaka University, Suita, Osaka 565-0871, Japan*

## Abstract

In this contribution, we give a brief survey of some elementary many body processes observable at surfaces. We begin the survey by discussing how the electron ground-state would behave and look like in real-space at surfaces. Next, we discuss how these electrons behave when they are perturbed by external fields characterized by ultrashort time scales. We follow this with a discussion of how the dynamics of electrons would then affect the motion of adsorbates on surfaces. Finally, we cite some possible technological applications utilizing this knowledge. We also discuss possible trends or directions of scientific research in this next century.
*Keywords*: Many body and quasi-particle theories; Electron density, excitation spectra calculations; Desorption induced by electronic transitions (DIET); Electron transport measurements; Kondo effect; Dilute Magnetic alloys; Metallic surfaces; Conductivity

## 1. INTRODUCTION

A recent and continuing trend in surface science is towards an understanding of the dynamical nature of surfaces. The basic rationale underlying this trend is as follows: Let us consider, *e.g.*, how dynamical processes proceed around us. A slight change (*e.g.*, induced by light irradiation) in the electronic states making up a solid surface interacting with atoms or molecules gives rise to a slight change in the position of atoms and molecules, which in turn initiates, further, a marked change in the electronic states. Eventually, the coupled electronic and atomic processes proceed to the final state on the surface. This may be properly regarded as characteristic of all dynamical processes occurring on surfaces, including chemical reactions. It is also a characteristic of all dynamical processes occurring around us, starting from those involving life forms and extending to other complex systems. Thus, in order to deepen our understanding of the dynamics of complex systems, it is necessary to clarify the fundamental mechanism behind the dynamics of each of the elementary processes. The most important breakthrough we can achieve towards a thorough understanding of the dynamics occurring around us would come from an accurate understanding of the elementary processes, in which mass, charge, and energy transport play important roles.

With recent advances in experimental techniques in the field of surface science, we are now at the stage where we can prepare well characterized solid surfaces, which, in a sense, serve as *playgrounds* for physicists. The solid surface provides us with a stage to study the dynamics of complex systems, where state transitions of the corresponding electron system are closely connected with the changes of atomic and molecular motion on various scales of magnitude with respect to time, space, and energy. For this reason, it is not only interesting but also necessary and important to study the excited as well as the ground states of the electron system constituting the system of a surface in interaction with atoms and molecules.

We begin our brief survey by considering the dynamics of surface electrons as the temperature is lowered to 0 K (the electron ground state!) in §. We then consider the dynamics of electrons perturbed by external fields characterized by ultrashort time scales in §. We then continue by considering how the dynamics of atoms or molecules adsorbed on surfaces are affected by the ultrafast electron dynamics.

## 2. A PHYSICAL GLIMPSE OF HOW ELECTRONS AT SURFACES LOOK AS $T \to 0$ K

### *2.1. The Kondo Effect and The Resistance Minimum Phenomenon - A Brief History*

The electric resistance is related to the amount of electrons (back) scattered from defects and the vibrations of the atoms (phonons), which effectively hinders the motion of the electrons through the crystal. As the temperature of a material (*e.g.*, a pure metal) is lowered, the vibrations of the atoms (phonons) that make up the material become small, and it becomes easier for the electrons to travel through the material. Thus, usually, the electric resistance of a material decreases as the temperature is lowered. However, due to static defects (which are not affected by the temperature) in the material, the resistance saturates as the temperature is further lowered below some critical temperature ($\approx 10$ K). The value of the low-temperature resistance depends on the number of defects in the material. Adding defects increases the value of this "saturation resistance" without changing

*Electronic address: kasai@dyn.ap..eng.osaka-u.ac.jp.; URL: http://www.dyn.ap.eng.osaka-u.ac.jp.
†Also at Japan Science and Technology Corporation, Kawaguchi, Saitama 332-0012, Japan.

the character of the temperature dependence. However, the temperature dependence of the resistance changes dramatically when magnetic atoms, e.g., Fe, are added. Rather than saturating, the electric resistance increases as the temperature is lowered further.

The observation of a resistance minimum in some metals, as a function of temperature $T$, one manifestation of the effect of magnetic impurities, has been known as early as the 1930s. Meissner and Voigt [1] discovered that instead of decreasing monotonically as one would expect [2], the electric resistance $R$ of Mg, as with other samples they have tested, has a shallow minimum occurring at a low temperature $T_{\rm K}$ ($O$(10 K)), now widely known as the Kondo temperature. The Mg sample showed a higher electric resistance at the temperature $T$ = 1 K, than resistance at $T$ = 4 K, *i.e.*, $R(T = 1\ {\rm K}) > R(T = 4\ {\rm K})$. Following Meissner and Voigt, de Boer *et al.* [3] found that the characteristic $R$ *vs.* $T$ curves of several other samples also showed minima. Why?—When?—How?—does this "resistance minimum phenomenon" occur? These were probably the questions occupying the minds of the condensed matter physicists at that time. Later, it was found that the occurrence of an electric resistance minimum was due to the presence of magnetic impurities. Typical examples are when trace amounts of Fe, Mn and Co are found in the samples of Cu, Ag, and Au. (For more examples, we refer the readers to, *e.g.*, [4–8].) However, because resistance minima were observed even for minute quantities (*e.g.*, in units of parts per million) of magnetic impurities, it was difficult to prepare samples and perform experiments that would, without a trace of doubt, establish the presence of the magnetic impurities as the origin of the resistance minimum observed. To make matters even worse, metals with nonmagnetic impurities like Sn also exhibited a resistance minimum. Sarachik *et al.* [9] found the solution. By measuring the electric resistance of samples prepared by Clogston *et al.* [10] they found that there was a one-to-one correspondence between the existence of a localized magnetic moment and the existence of a resistance minimum. The weak magnetic impurity concentration dependence of the temperature of the minimum resistance and the scaling of the low temperature resistance with impurity concentration indicated that this phenomenon arised from the interaction of the sea of conduction electrons (mobile electrons that behave like a sea—Fermi sea—that fills the entire sample) with isolated magnetic impurities, and not from the impurity-impurity interactions [4, 5]. A typical example of this so-called *resistance minimum phenomenon* is shown in Fig. 1. (For a more thorough review of the experimental facts that were available until 1964, we refer the readers to the paper by van den Berg [12].)

The mystery enshrouding the resistance minimum phenomenon persisted for over 30 years. A very significant advance in the theory of magnetic impurities was an explanation of this phenomenon by J. Kondo in 1964 [13], 30 years after it had been observed experimentally. As infererred above, the electric resistance is related to the amount of back scattering from defects, which hinders the motion of the electrons through the sample crystal. Usually, one can readily calculate the probability with which an electron will be scattered when the defects are small. For larger defects, one could usually perform the calculation using perturbation theory—an iterative process in which the answer is usually written as a sum of a series of smaller and smaller terms. However, in 1964, Kondo, when he considered the scattering from a magnetic impurity that interacts with the spins of the conduction electrons, found that the second term in the perturbation calculation could be larger than the first. Kondo showed, using perturbation theory, that many body effects due to dynamical interactions and scattering of the conduction electrons at the Fermi level (all the states in the Fermi sea with energies below the so-called Fermi level are occupied, while the higher energy states are empty) by a single localized magnetic impurity with an associated local spin moment leads to a $-\ln T$ contribution to the resistance. The $-\ln T$ term increases at low temperatures and when this term is included with the phonon contribution (scattering of the conduction electrons due to the vibrations of atoms—phonons—in the sample) into the resistance, it is sufficient to explain the observed resistance minimum (Fig. 2).

The occurrence of a resistance minimum is connected with the existence of localized magnetic moments on the impurity atoms. As mentioned above, the criterion for a localized moment is a term in the magnetic susceptibility inversely proportional to the temperature, with a coefficient proportional to the density of magnetic atoms as predicted by (Pierre) Curie's law [6–8]. The moment of the free atom is determined by Hund's rules [6–8], which in turn are based on considerations of the intra-atomic Coulomb (and, to a lesser degree, spin-orbit) interactions. Where a resistance minimum is found, there is inevitably a local moment. Kondo has shown that the anomalous high scattering probability of magnetic atoms at low temperatures is a consequence of the dynamic nature of the scattering by the exchange coupling and of the sharpness of the Fermi surface at low temperatures. Hence the solution of a long-standing puzzle!

## *2.2. The Electron Ground State is a Singlet!*

However, there were difficulties with the theory. Note that because $\ln T$ terms diverge as $T \to 0$, Kondo's perturbation calculations could not be valid at low temperatures. Although Kondo's theory correctly describes the observed upturn of the resistance at low temperatures, it also makes the unphysical prediction that the resistance will be infinite at even lower temperatures. It turns out that Kondo's result is correct only above a certain temperature, which became knows as the Kondo temperature $T_{\rm K}$. A more comprehensive theory was needed to explain questions such as—What would be the actual low temperature ($T \to 0$) behavior of the electron systems showing

resistance minima, *i.e.*, what would be the ground state of the electron system of a dilute magnetic alloy? The search for such a theory opened a new and fascinating field of research for many body condensed matter physics, and became known as the *Kondo problem* [14–20].

The results of the pertubation calculations of Yosida [21] and Okiji [22], who showed that the results of Yosida's perturbation calculation [21] persist even after considering higher order terms in the pertubation calculation, for the susceptibility suggest that the localized spin falls into a *many-body singlet ground state* (Fig. 3). Furthermore, they concluded that the reason why earlier investigators, who also performed perturbation calculations, got unphysical results—the logarithmic divergence—was because they disregarded the existence of the singlet bound state and, instead, started with degenerate localized spin states .

In Fig. 3 we illustrate what happens when a magnetic impurity (with an associated magnetic moment/spin, analogous to having a bar magnet whose configuration is described by being spin "up" ($\uparrow$) or spin "down" ($\downarrow$), localized at the position of the impurity), interacts with the spins of the conduction electrons. To aid the illustration, we adopt the energy scheme of the Anderson model (the simplest model of a magnetic impurity, introduced by Anderson [34] in 1961) to describe the energy structure of a magnetic impurity interacting with a sea of mobile (conduction) electrons—Fermi sea (blue). The Anderson model assumes that the impurity is described by a localized state (e.g., the $d$-orbital) occupied by a single electron with energy below the Fermi energy $E_{\rm F}$ of the metal. $E_d$ indicates the energy of the localized state of the magnetic impurity when it is occupied by a single electron of either spin $\uparrow$ or spin $\downarrow$ (red). Occupancy of the localized state by another electron of opposite spin results in an increase in the corresponding energy level by $U$, the Coulomb energy. Removing an electron from the localized state requires at least $|E_d|$. Although it is classically forbidden to take an electron from the localized impurity state without feeding energy into the system, in quantum mechanics, the Heisenberg uncertainty principle allows such a configuration to exist for a very short time—$\approx h/|E_d|$, where $h$ is Planck's constant. Thus, the spin $\uparrow$ electron initially occupying the the energy level $E_d$ (a), may tunnel out of the impurity site to briefly occupy a classically forbidden "intermediate state" (b) outside of the impurity. Within the time scale $h/|E_d|$, another electron must tunnel from the Fermi sea back towards the impurity (c). However, the spin of this electron may point in the opposite direction. Thus, the initial and final states of the impurity may have different spins. This spin "flipping" or spin exchange qualitatively changes the energy spectrum of the system (d). The Kondo effect is thus produced by a combination of such events taken together, and this results in the appearance of an extra resonance level/a new state (the singlet bound state) at the Fermi energy—- known as the Yosida-Kondo resonance (Yosida singlet state) [21, 22] (d). Thus, we can see, taken as a whole (the system consisting of a magnetic impurity ineracting with the conduction electrons), the localized spin of the magnetic impurity does not survive upon interaction with the spins of the conduction electrons, at very low temperature—the low temperature spin of the system is neither spin $\uparrow$ nor spin $\downarrow$, as earlier assumed by earlier investigators. We now know, from hindsight, that the low-temperature increase in the resistance is an indication of the existence of this new state. Such a resonance state is very effective at scattering electrons near the Fermi level, and since the same electrons are responsible for the low-temperature conductivity of a metal, the strong scattering greatly contributes to the electric resistance.

From then on, starting with the ground state properties and resistance near absolute zero temperature, several physical quantities were clarified with more detailed studies [23–25]. Starting with Wilson's [14] solution which was valid for all temperature range, one after the other, exact solutions [16, 26, 27] to the two basic models used to study dilute magnetic alloys, *viz.*, the $s$-$d$ model [4, 19, 21, 22, 28–33] and the Anderson model (Fig. 3(a)) [5, 34, 35], were discovered in the early 1980s. These studies confirmed the generality of earlier perturbation theory results, and further resolved fundamental problems related to the Kondo effect relevant to a single magnetic impurity. Since then, numerous systematic and extensive studies [18, 36–39] of a variety of physical properties, *e.g.*, magnetism and superconductivity, and of heavy fermion systems were made, as an extension of the Kondo impurity system. Other fields of condensed matter physics, *esp.*, the studies of high transition temperature $T_C$ superconductivity have greatly benefited from the results of these studies.

For more information on researches carried out in magnetism, we refer the readers to the articles by Bader [40], Goedkoop [41], and Shen *et al.* [42] in this issue of Surface Science.

One important thing to note about the Yosida-Kondo resonance (Yosida singlet state) is that it is always "on resonance", as it is fixed at the Fermi level. Although the system may start with the energy of the localized state of the magnetic impurity ($E_d$ in Fig. 3) located very far from the Fermi level, dynamical interaction between the conduction electrons and the localized spin at the magnetic impurity changes the energy spectrum of the system so that it is always on resonance. The only requirement for the Yosida-Kondo resonance (Yosida singlet state) to appear is that the system be cooled to temperatures sufficiently below the Kondo temperarture $T_{\rm K}$.

Because many electrons are involved in the spin-flip processes (as decribed above and in Fig. 3) to build the Yosida-Kondo resonance, the Yosida-Kondo resonance state is a *many-body singlet bound state*. Also note that each of the electrons that has previously interacted with the same magnetic impurity (the so-called Kondo cloud) contains information about the same magnetic impurity, each electron effectively contains information about the

other electrons (the electrons making up the Kondo cloud interact with each other via the localized spin at the magnetic impurity). Thus, we could also say that the Kondo effect is a strongly correlated, many body phenomenon/effect.

The holy grail for research on the Kondo effect is the quest for a possible means of measuring and controlling the Kondo cloud. Another equally important quest is to understand how such a many body quantum state evolves in time? In the next section, we will discuss how Surface Science made another important contribution to this quest, by allowing us to visually observe the Yosida-Kondo peak, and of course, the accompanying Kondo cloud.

### *2.3. The Real-Space Image of the Yosida-Kondo Peak*

In 1993, almost 30 years after Kondo had solved the puzzle regarding the resistance minimum phenomenon, Crommie *et al.* [43] studied the behavior of an Fe atom adsorbed on Cu(111) surface with the aid of a scanning tunneling microscope (STM). Operating the STM at constant-current mode, and the temperature $T = 4$ K, they scanned a region of the surface 130Å×130Å in area with the Fe adatom centered in this region. The corresponding STM image of the region showed a central main peak structure at the position of the Fe adatom, and concentric standing waves around it (*cf.*, Fig. 4(a)). These concentric standing waves arise as a result of the interaction/interference between the conduction electrons scattered by the Fe adatom. The height of the standing wave is distinguishable to within 0.01Å, which gives us an idea of the high degree of resolution attainable with STMs! By modelling the Fe as a cylindrically symmetric scattering potential, they were able to derive an expression for the change in the local density of states (LDOS) at the Fermi level $E_{\rm F}$ surrounding the Fe atom, and reproduce the standing wave structure observed *far from the Fe* (with surface lateral distances $r$[Å] $>$ 20Å from Fe ) in the STM image (*cf.*, Fig. 4(b)). In addition to this, they also measured the corresponding density of states distribution ($dI/dVvs.V$ curve).

Since the Fe/Cu(111) system is a *classic* example of a dilute magnetic alloy showing the Kondo effect, these data, as well as the *sharp peak structure* observed at the position of the Fe, motivated Kasai *et al.* [44–46] to propose observing the Kondo effect, in particular the Yosida-Kondo peak (Yosida singlet state) in real space, with the aid of the STM. A few years later, independent [47] of the works of Kasai *et al.* [44–46], Manoharan *et al.* [48] actually succeeded in obtaining a real-space image of the Yosida-Kondo peak for the system Co/Cu(111) (*cf.*, Fig. 1(c) of [48]), using the same procedure suggested earlier by Kasai *et al.* [44–46] (Fig. 6).

Madhavan *et al.* [49] and Li *et al.* [50] measured the corresponding differential conductance $dI/dV$ *vs.* bias voltage $V$ spectra for a magnetic atom on a metal surface—Co/Au(111) and Ce/Ag(111), respectively. Their results show that near the magnetic atom, the corresponding $dI/dVvs.V$ curve shows either an asymmetric or a symmetric dip structure about the Fermi level ($V = 0$). Analysis of their data suggests that the energy width of the observed dip structure is directly related to the Kondo temperature of the corresponding system (*cf.*, *e.g.*, Fig. 5 [49]).

For more details on the utilization of the STM and its main achievements, we refer the readers to the articles by Plummer *et al.* [51], Crommie [52], Hasegawa *et al.* [53], and Ho [54] in this issue of Surface Science, and also [55–57].

In Fig. 6 we show the calculated results [44–46], for the spatial distribution of the tunneling current $I(\mathbf{R}) = I(x, y, z)$ for the case when the STM tip is placed at a distance $z = 4.0$Å from the surface, and scanned along the surface. In the vicinity of the Fe atom ($r \leq 5$Å, Fig. 6(a)), we can see a narrow peak structure, the Yosida-Kondo peak, which grows large with decreasing temperature. This can be interpreted as due to the relaxation of the electron system to the ground state (Yosida singlet state), as $T \rightarrow 0$, and the narrow peak is the spatial manifestation of the ground state wave function. In the region $r > 5$Å (Fig. 6(b)) we can observe some oscillations (Friedel oscillations) in $I(\mathbf{R})$. (Note that the ordinates of Figs. 6(a) and 6(b) differ by three orders of magnitude). We can see that there are some regions of $r$ where $I(\mathbf{R})$ increases in amplitude as $T \rightarrow 0$, and some regions of $r$ where $I(\mathbf{R})$ does not vary much with $T$.

In Fig. 7 we show the calculated results [44, 46] for the variation in STM tip height from the surface, when we operate the STM at constant current mode and scan along the surface. The qualitative features of the calculated results are comparable with experimental results for the STM tip height variations (*cf.*, Fig. 4(b)) [43]. The peak height of $\approx 0.5$Å is of the same order as that of experimental results [43]. Similarly, the standing wave has an amplitude variation of ($\approx 0.02 \pm 0.01$Å) and a period ($\approx 15$Å) that resembles the experimental data. We note that the period of the standing wave is closely related to the Fermi wave number (corresponding to the above-mentioned Fermi level) $k_{\rm F}$.

Thus, as mentioned earlier, the surface has provided us with a playground to study the Kondo effect, in particular, the Yosida-Kondo resonance (Yosida singlet state) and the accompanying Kondo cloud. Because of the existence of conduction electrons localized at the surface (surface electron state, Fig. 9) and the ability of surface scientists to probe the electrons at surface with an STM, we are now at the stage where we could measure and visulize the Kondo cloud. With further developments like the ability to probe the surface with the STM under varying temperatures and magnetic fields (*cf.*., further discussion below regarding the Kondo temperature), we will soon be able to understand how such a many body quantum state evolves in time?

# 3. A FEW WORDS ON THE KONDO TEMPERATURE $T_K$

At present, as far as we know, there is no way one can predict what the Kondo temperature $T_K$ would be for a particular system. However, as discussed in §?? and §?? (for more details also *cf.*, *e.g.*, [44–46]), this should be measurable from the $dI/dV$ spectra. The width of the resonance at near the Fermi level is $\approx 2k_B T_K$. However, if one does not have a reproducible $dI/dV$ spectra, one could still experimentally estimate the value of $T_K$ from the temperature dependent $I$ *vs.* $r(=\sqrt{x^2+y^2})$ curve. For systems with low $T_K$, *e.g.*, Fe/Cu(111) ($< 20$ K) and Co/Au(111) ($\approx 55$ K), the magnitude of the peak structure at the position of the magnetic adatom would decrease by 50% upon an increase in temperature from 0 to 100K. For systems with high $T_K$, *e.g.*, Ce/Ag(111) ($\approx 250$ K), the magnitude of the peak structure at the position of the magnetic adatom would decrease by no more than 10% upon an increase in temperature from 0 to 100K. Thus, one would have reached $T_K$ when the peak structure is $\approx 75\%$ of that at 0 K. Alternatively, one could monitor the width of the $dI/dV$ spectra and determine how the resonance width changes with temperature $T$. For temperatures $T < T_K$, the resonance width slowly increases ($\propto T^2$) as you sweep the $T$ from $T << T_K$ up to $T_K$. Upon crossing $T_K$, one observes an abrupt change in the resonance width. Further increases in $T$ causes the resonance to become negligible. Another way of verifying that we are actually seeing the real-space image of the Yosida-Kondo peak is to study how it changes upon the application of an external magnetic field [65], which is also experimentally feasible [66, 67].

Thus, we see the manifestation of the Kondo effect in the corresponding STM image of a magnetic atom on a metal surface, or the corresponding spectra, *via* the electron tunneling between the STM tip and the localized orbitals of the magnetic atom, and between the STM tip and the states of metal conduction electrons scattered by the magnetic impurity atom. We hope that with further studies, we can gain a better understanding of how a magnetic atom behaves on a metal surface. With this new ability to *observe the Kondo effect in real space* one of our long-standing dreams from the research of dilute magnetic alloys may come true.

# 4. ULTRAFAST ELECTRON DYNAMICS STUDIED BY TIME-RESOLVED TWO-PHOTON PHOTOEMISSION SPECTROSCOPY

## *4.1. Femtosecond Time-Resolved Two-Photon Photoemission Spectroscopy*

How do electrons in the metal surface respond when perturbed with external fields on ultrashort time scales? This is a fundamental question, since ultrafast dynamical processes involving electrons affect chemical reactions and optical responses at the surfaces of metals. Let us consider, for example, photon-stimulated desorption. Initially, we photoexcite the electrons of the metal surface at/on which atoms and molecules (adparticles) are adsorbed. Subsequently, the adparticles gain enough kinetic energy to desorb from the surface because of energy and charge transfers between the metal and the adparticles due to electronic transitions [68, 69]. Since the excited electrons relax in a femtosecond ($10^{-15}$ second) time scale, however, it is difficult to ascertain the dynamics of electrons in such ultrafast surface processes. Fortunately, recent progress in femtosecond laser technology has revolutionized the study of ultrafast dynamics. An effective experimental method for studying ultrafast electron dynamics is time-resolved two-photon photoemission (time-resolved 2PPE or "TR2PPE") spectroscopy.

A schematic diagram of TR2PPE spectroscopy is given in Fig. 8(a), the metal surface is irradiated with pump and probe laser pulses, and then the intensity of the photoelectron emitted from the surface is measured as a function of the photoelectron energy and pump-probe delay time (TR2PPE spectrum). An energy diagram of a 2PPE process is shown in Fig. 8(b). First a pump photon excites an electron from an initial state below the Fermi level into an intermediate state above the Fermi level (hence a hole is excited/created at the initial state level). The temporal evolution of the electron density in the intermediate state can be affected by electron hopping between the substrate metal and the adparticle and various scattering processes, *e.g.*, electron-electron and electron-phonon scattering and electron scattering at impurities and defects. As a result, the electron density decreases and the electron system loses coherence (phase information). Next a probe photon excites the electron from the intermediate state into a final state above the vacuum level, and hence the electron is likely to be emitted from the surface. This process can be described by, *e.g.*, the optical Bloch equations or the Liouville-von-Neumann equations [70] .

### *4.2. Photoinduced Dynamics of Electrons in Localized States at Surfaces*

When an electron moves in front (immediately outside) of a clean metal surface (Fig. 9), the motion of the electron is affected by the image potential which accounts for an attractive force towards the surface due to dielectric response of other electrons in the vicinity of the surface. As a result, the electron can be trapped between the image potential and the surface, which acts like a hard wall barrier if there exists the projected band gap at the surface. Hence, localized electron states called *image states* may exist in front of the surface, which form a Rydberg-like series below the vacuum level $E_V$ (Fig. 10). Because of their accesibility, image states provide a useful system to study ultrafast electron dynamics both theoretically and experimentally.

In clean Cu(100), the vacuum level is located at the center of the projected band gap, and image states with various quantum number $n$ exist just below the vacuum level (the upper panel of Fig. 10). The wave functions of these states spread several nanometers out of the surface, and the lifetimes of these states are of the order of $O(10 - 1000$ fs) long [77]. Irradiating the surface with a femtosecond laser pulse can result in excitation of an electron wave packet oscillating in front of the surface (quantum beats), when the full width at half maximum (FWHM) of the laser pulse is shorter than 100 fs (the FWHM of the energy spectrum is larger than 13 meV and hence more than two image states are included in this energy range), as 2PPE processes via various image states interfere with each other. Sakai *et al.* [78] theoretically demonstrated a procedure for analyzing the corresponding TR2PPE spectrum to aid in the understanding of the dynamics of electrons, which provides information on the temporal evolution of the phase of the probability amplitude, and thereby on the motion of the electron wave packets in the *space domain* (Fig. 11).

In clean Cu(111), the vacuum level is located just above the top of the projected band gap (lower panel of Fig. 10). As a consequence, $n \geq 2$ image states are in resonance with the bulk states and the peak structure due to the states in the 2PPE spectrum becomes indistinct, and the $n = 1$ image state has a lifetime $\approx 10$ fs [83]. Moreover, a localized state called *Shockley state* exists at the surface [76, 79, 80]. The $n = 1$ image state of Cu(111) is an attractive target for researchers of ultrafast electron dynamics in metals because the 2PPE process via this state is well-defined, although complicated. The 2PPE (normal emission) from Cu(111) occurs via the following two processes— (*i*) Process (SS), where an electron in the Shockley state with $k_{//} = 0$ ($k_{//}$ stands for the component of the wave vector parallel to the surface) below the Fermi level is first excited into the image state with $k_{//} = 0$ by a pump photon, and then, subsequently, it is further excited into a free electron state above the vacuum level. (*ii*) Process (IS), where an electron in a state with $k_{//} \neq 0$ is first excited by a pump photon (hence a hole with $k_{//} \neq 0$ is excited), and then, subsequently, electron transfer into the image state with $k_{//} = 0$ occurs accompanied by scattering of the photoexcited electron or the hole by the cold Fermi sea, and finally the electron in the image state is excited by the probe photon.— Process (SS) accounts for tbe peak in the 2PPE energy spectrum at an energy position obtained by adding the pump and probe photon energies to the energy level of the Shockley state, while process (IS) accounts for the peak at an energy position obtained by adding the probe photon energy to the energy level of the image state.

When the pump photon energy is not in resonance with the energy region between the image and Shockley states, relaxation of the electron excited from the Shockley state into the image state occurs in a time shorter than the intrinsic lifetime of the image state. As a result, the correlation trace at the SS-peak is not affected by lifetimes of either electrons or holes. On the other hand, the correlation trace at the IS-peak is affected by the lifetimes of the electrons and holes involved in the 2PPE process. Sakaue *et al.* [81] theoretically demonstrated that the effect of Coulomb interactions between electrons, which is important in the understanding of the TR2PPE spectrum of bulk states [82], is equally as important in the understanding of the TR2PPE spectrum of the image state (Fig. 12).

In Fig. 12, the increase in the lifetime of the electron in the image state can be explained by the reduction in the scattering probability of the electron by other electrons in the bulk, since the wave function of the image state is pushed away from the surface by Xe adsorption [84]. Here, what should be emphasized is that the lifetime of the photoexcited electron or the hole is longer in the experiment on the Xe/Cu(111) surface than that on the clean Cu(111) surface. The results show that the pump photon with a lower energy excites an electron and a hole into states with energies closer to the Fermi level, which have longer lifetimes as understood qualitatively from the Fermi liquid theory [85].

### *4.3. Optical Control of Dynamical Processes at Surfaces*

Extensive studies of ultrafast electron dynamics in metals by TR2PPE spectroscopy [86–91] and the theoretical analyses [92] of the experimental results obtained are gradually clarifying the mechanisms of the optical response of electrons in bulk states and localized states at metal surfaces. Possible next targets of these studies will be the development of methods to control dynamical processes involving atomic and molecular motions on surfaces by femtosecond laser pulses. Information like that presented in the previos section serve as helpful hints for controlling dynamical processes through the photon energy. Recent theoretical studies also predict the possibility of controlling dynamical processes by changing the pulse duration [82, 92]. Coherent control of these

processes, in which interference between laser pulses is applied, is an additional interesting theme for studying ultrafast dynamics [88? ].

# 5. ADSORBATE DYNAMICS INDUCED BY STM—CO DESORPTION FROM CU(111) AND ACETYLENE ROTATION ON CU(001)—

Continuing on and developing over the question we asked earlier in the beginning of §, we address the question how adsorbates (atoms/molecules on a solid surface) would respond, in turn, when the corresponding electron system is perturbed by some external fields and forced to make a transition from the ground state of the electron system to an excited state? What physical mechanism governs the motion induced? In what follows, we will consider the STM-induced desorption of a single CO from Cu(111) and acetylene rotation on Cu(001), and discuss the mechanism behind the corresponding adsorbate motion induced from a microscopic point of view.

## *5.1. CO Desorption from Cu(111)*

In 1998, by combining the atomic length scale spatial resolution of tunneling spectroscopy (TS) and the femtosecond time-scale temporal resolution of two photon photoemission (2PPE), Bartels *et al.* [86] were able to observe the motion of a single CO induced by *the tunneling of a single electron* from the STM tip to the metal substrate. The bonding of CO to Cu(111) is described in Fig. 13. The electron tunnels into the CO $2\pi^*$ orbital, thereby destabilizing the bonding of the CO to Cu(111) as indicated in Fig. 14. Bartels *et al.* [86] also determined the lifetime of the tunneling electron in the CO $2\pi^*$ orbital to be $0.8 - 5$ fs.

Hasegawa *et al.* [96] introduced a microscopic model to describe the physical mechanism leading to the abovementioned STM-induced motion of the CO, which we present below. For simplicity, we will consider only the center-of-mass (CM) motion of CO in the direction normal to the Cu(111), and neglect the hindered rotational motion and other internal degrees-of-freedom (DOF), *e.g.*, C-O bond stretching, *etc.*, and also the effect of the presence of the STM tip. We assume that the motion of CO along the direction normal to the Cu(111) corresponds to the motion of its CM along a Morse potential, whose structure is determined by the ground state energy of the CO/Cu(111) electron system. Starting with a CO adsorbed on the surface (Fig. 15 (a)), Hasegawa *et al.* [96] introduced a single electron, supposedly originating from the STM-tip, which occupies the $2\pi^*$ orbital of the adsorbed CO. This electron initially *already* occupying the $2\pi^*$ orbital of the adsorbed CO then, subsequently, transfers/tunnels to the metal substrate (Fig. 15 (b)). Because electron hopping/transfer between the $2\pi^*$ orbital of the adsorbed CO and the metal orbital depends on the distance between the CO and the metal surface, the tunneling of the electron from the $2\pi^*$ orbital of the adsorbed CO to the metal substrate may induce the excitation of different CO-surface vibrational stretching modes. When the CO-surface stretching mode in the neutral CO-surface potential is excited to a state with a corresponding energy greater than the adsorption energy of CO on Cu(111), CO desorption/relocation from/on Cu(111) occurs, otherwise, the CO stays in place.

With the microscopic model described above, Hasegawa *et al.* [96] were able to reproduce the low probability of CO desorption induced per tunneling electron observed experimentally ($\approx 10^{-11}$), as well as the experimentally observed isotope effects. Moreover, Hasegawa *et al.* [96] gave an estimation of what the mean translational energy of CO would be upon desorption—$\approx$ 10 meV. This value is very small compared to the mean translational energy of $\approx 2$ eV for a $H^+$ desorbing (induced by electron-beam bombardment) from a W surface [97], and a mean translational energy of $\approx 100$ meV for NO desorbing (induced by light irradiation) from a Pt surface [98]. It seems to give us an indication of the energy necessary/relevant/appropriate for manipulating individual adsorbates on surfaces by STM. And also an indication of how effective utilizing STM induced dynamics would be to make structures on surfaces, and carry out a step-by-step realization of chemical reactions on surfaces [99, 100].

By extending the microscopic model described above, Hasegawa *et al.* [101, 102] were also again able to reproduce the ultra low probability ($\approx 10^{-12}$) of $C_2HD$ rotational motion induced per tunneling electron experimentally observed by Stipe *et al.* [103], for the case when the C-H bond is initially under the STM tip. With the C-D bond initially under the STM tip, the corresponding probability of $C_2HD$ rotational motion induced per tunneling electron is one order higher ($\approx 10^{-11}$).

Further extensions of these models, to attain quantitative agreement with experimental results would involve the actual total energy calculations to determine the actual orbitals involved and the activation barriers (*cf.*, *e.g.*, [104–109]). From these calculations, one could, *e.g.*, calculate the STM image of the $C_2H_2$ adsorbed on Cu(100) [109], and distinguish whether the STM manipulation mode—pulling, sliding, or pushing—from the feedback loop signal [107].

# 6. OUTLOOK

Significant contributions from many researchers in the field of condensed matter physics—Starting with the observation of a resistance minimum in some metals, in

the early 1930s; the recognition that this minimum was a manifestation of many body effects, *i.e.,* the Kondo effect, which results from the interaction between a local magnetic moment associated with a spin and the conduction electrons of the host metal in dilute magnetic alloys; and our present understanding of this physical phenomenon—not only enriched the field in terms of content, the achievements also served as inspirations to other fields of research. The invention of the scanning tunneling microscope by G. Binnig and H. Rohrer in 1981 [110], also had a similar effect. Not only did it contribute to a clearer understanding of the structure of clean and adsorbate-covered surfaces, it has also become a necessary tool in the investigation and understanding of the physical properties of (associated with) atom-size regions, and in other fields as well. Five years later, the STM was joined in 1986 by the atomic force microscope (AFM) [111], and its versatility is also finding uses in terms of mapping the surfaces of solids under gaseous or liquid conditions, and even in producing images of biological molecules.

In §, we pointed out that as a result of recent achievements by both the theoretical and experimental studies, we are now in a stage where it might actually be possible to observe *a real space image of the electron ground state (Yosida-singlet), the Yosida-Kondo peak.* Recall that the origin of the Kondo problem was that, until the works of Yosida [21] and Okiji [22], perturbation calculations always started with the wrong ground state. In § and §, we mentioned that by combining the temporal (femtosecond time scale) resolution of time-resolved two-photon photoemission (TR2PPE) spectroscopy and the spatial (atomic length-scale) resolution of STM, together with scanning tunneling spectroscopy (STS), we have now within our means a powerful tool to induce and observe ultrafast dynamics of electrons, atoms, and molecules, and also the ability to manipulate and construct different atomic structures on the surface (as discussed in § and §). Numerous achievements have been made with the STM, as reported in the literature. Some examples are—the ability to observe the surface charge density distribution; the observation and study of atomic or molecular adsorbate-surface systems, steps, defects and vacancies; atomic-scale manipulations, nanolithography, nanofabrication (construction of quantum corrals [43, 48], atom-size bridges [112–115], *etc.*); STM induced dynamics (desorption from surface, rotation or dissociation on surface); and luminescence. Even biology has found a use for STMs, *e.g.,* DNA sequencing with an STM. All these achievements, regardless of the scientific field of research involved, were made possible by having an actual image of a natural phenomenon that occurs in the atomic or molecular level. Thus, it would be desirable to have a deeper understanding of the physical mechanism behind each STM image, and STM related phenomena—*e.g.,* How is quantum transport of electrons through an atom-size bridge affected by the shape of the constriction [116]? To what [117] can we attribute the deviation of the conductance through an atom-size point contacts made from STM-tips [112] from the universal value of $G_0 = 2e^2/h$? How do many body effects (electron-electron scattering) manifest in the corresponding conductance through an atom-size point contacts made from STM-tips [118–121]?

So what does the future have in store for us [122]? One answer would be Nanotech [123], where materials to be studied will measure in the range of 1 to 100 nanometers (for reference, a Cu measures 0.25 nanometers across). As Ward Plummer [51] would say—Whoever controls the materials controls the science and technology. So what will the future materials be? What will replace the silicon or the silicon-based computers? Optical computers?—Understanding ultrafast dynamics(§) will surely help in the development of this technology. Molecular computers [124], where individual molecules act like switches, wires and even memory elements; where instead of high current or no current representing bits 0 and 1, we use, the orientation [125] of the molecule with respect to the surface?—We would surely benefit from an understanding of adsorbate dynamics(§). How about DNA computers [126, 127], or quantum computers, where we use the internal degrees of freedom of individual atoms? Even increasing the capacities of magnetic data storage devices [128, 129] would require knowledge of how magnetic particles interact with each other when jammed together in a very small region (Kondo lattice, *cf., e.g.,* [20]).

Obviously, controlling things on the atomic scale is not a real big problem. It is only a matter of time before we perfect the technique, be it by using an STM, an AFM, a laser tweezer, or some combination of these. Who knows, some more ingenius method might even be discovered along the way. However, being able to observe the atoms that make up surfaces, or being able to manipulate individual atoms, by itself, will not lead to technological application. The next big question would be—How do we make these atoms and molecules come together to build large scale functional devices/materials? How can we take advantage of the inherent products/properties of naturally occurring elementary processes around us to create functional structures?

Nature, most probably, has all the answers. We, living things, for example, are built by natural elementary processes that operate at infinitesimally small scales, and yet functional structures like whales and redwoods exist. Thus, it is not really suprising to observe that recent developments in large scale integration of new devices are getting their hints from processes found in living organisms. It would not be far into the future when we will be able to custom design processes (reactions) much *like those occurring in nature.* We must remember that every time we take away something from nature, nature always has a means exacting her toll on us in turn. Thus, big challenge would be—How do we continue to improve our way of life and still maintain our balance with nature? How should we design processes, such that by-products would not be the cause of a new disease, the extinction

of a species of organism, or the degradation of our environment? Most likely, we would have to find means of designing processes based on naturally occurring processes that are not only user-friendly, but also nature (environment) friendly.

In any event, we again find ourselves in the earlier stages of a new quest with many unanswered questions. However, we believe that further significant contributions and new discoveries are on the way. In a recent article, Diño *et al.* [125] mentioned the significance of understanding the mechanisms behind the dynamics of atom/molecule-surface reactions. We hope that with this article we have shown that the dynamical processes involving the surface electrons of an adsorbate-surface system are equally as interesting and important. As a result of the dynamics of the surface electrons, we now have a means with which we could *actually observe* a physical phenomena that would otherwise not be possible in the bulk. As the saying goes—*A picture says more than a thousand words.* Furthermore, coupled with recent developments in computation techniques for doing first principles electron structure calculations, we now have within our means a powerful tool for systematic analysis of the fundamental mechanism behind dynamical processes occurring at surfaces. And we believe that in order to gain a full understanding of physical phenomena occurring around us in nature, investigations involving surface physical properties such as those presented here are necessary and important.

## Acknowledgments

We gratefully acknowledge the tremendous effort devoted by our collaborators Dr. Hiroshi Nakanishi, Dr. Mamoru Sakaue, and Dr. Kazuhiko Hasegawa in helping us prepare this manuscript, and for sharing with us their opinions on how to prepare this manuscript. We would also like to acknowledge useful discussions with Dr. Atsushi Fukui and Dr. Yoshio Miura. We would also like to thank Prof. Mike Crommie, Dr. Donald Eigler, Prof. Wilson Ho, Prof. Wolf-Dieter Schneider, and Prof. Ludwig Bartels, who were always willing to explain that are and can be obtained in their experiments, and also for sending us some of the original figures that appear in this article. And last, but not the least, special thanks to Dr. Charles Duke and Prof. Ward Plummer, who initiated and devoted a lot of their time into making this special issue of Surface Science happen. Our original works cited here are partly supported by the Ministry of Education, Culture, Sports and Science and Technology of Japan through Grants-in-Aid for Creative Basic Research (No. 09NP1201), COE Research (No. 10CE2004), and Scientific Research (No. 11640375) programs, and by the Japan Science and Technology Corporation (JST), through their Research and Development Applying Advanced Computational Science and Technology program. Some of the calculations in our works cited here were done using the computer facilities of the Japan Science and Technology Corporation (JST), the Institute of Solid State Physics (ISSP) Super Computer Center (University of Tokyo), the Yukawa Institute (Kyoto University, the Center of Computational Physics (Tsukuba University), and the Cybermedia Center (Osaka University). W.A.D. gratefully acknowledges Fellowship grant from the Japanese Society for the Promotion of Science (JSPS), under their Postdoctoral Fellowship Program for Foreign Researchers, and financial support from the Inoue Foundation for Science (Inoue Research Award for Young Scientists).

## A few words of explanation on references

In covering subjects like the Many Body Effects, for which there is a vast literature, the problem of which references to cite is an especially difficult one. We have found no good solution to this problem, but we have adopted the following guiding principle—The papers have been selected as ones most closely related to the particular subject we are discussing, or the ones most familiar to us. Inevitably, much interesting related work will appear to have been overlooked (we sincerely apologize to any contributors to the field who feel that this applied to their work). We do, however, strongly encourage the readers to use the cited references as "seed" references. Used in this way, together with the reference list of the cited review articles, they should be able to build up a comprehensive list to the whole field or any part of it which is of particular interest to them.

[1] W. Meissner and G. Voigt, Messungen mit Hilfe von flüssigem Helium XI: Widerstand der reinen Metalle in tiefen Temperaturen (Meaurements with Liquid Helium XI: Resistance of Pure Metals at Low Temperatures), Ann. Phys. (Germany) **7** (1930) 761, 892.

[2] J.M. Ziman, Electrons and Phonons: The Theory of Transport Phenomena in Solids, (Oxford, Clarendon, 1963).

[3] W.J. de Haas, J. de Boer, and G.J. van den Berg, The electrical resistance of gold, copper, and lead at low temperatures, Physica **1** (1934) 1115.

[4] J. Kondo, Theory of Dilute Magnetic Alloys, in: Solid State Physics, Vol. 23, Eds. F. Seitz, D. Turnbull, and H. Ehrenreich (Academic Press, New York, 1969) p. 183.

[5] A.J. Heeger, Localized Moments and Nonmoments in Metals: The Kondo Effect, in: Solid State Physics, Vol. 23, Eds. F. Seitz, D. Turnbull, and H. Ehrenreich (Academic Press, New York, 1969) p. 283.

[6] N.W. Ashcroft and N.D. Mermin, Solid State Physics, (Saunders College Publications, Philadelphia, 1976).

[7] W.A. Harrison, Solid State Theory (Dover Publications, Inc., New York, 1979).

[8] C. Kittel, Introduction to Solid State Physics, 7th edition (John-Wiley & Sons, Inc., New York, 1996).

[9] M. Sarachik, E. Corenzwit, and L.D. Longinotti, Resistivity of Mo-Nb and Mo-Re Alloys Containing 1% Fe, Phys. Rev. **A135** (1964) 1041.

[10] A.M. Clogston, B. Matthias, M. Peter, H.J. Williams, E. Corenzwit, and R.C. Sherwood, Local Magnetic Moment Associated with an Iron Atom Dissolved in Various Transition Metal Alloys, Phys. Rev. **125** (1962) 541.

[11] J.P. Franck, F.D. Manchester, and D.L. Martin, The specific heat of pure copper and of some dilute copper+iron alloys showing a minimum in the electrical resistance at low temperatures, Proc. Roy. Soc. (London) **A263** (1961) 494.

[12] G.J. van den Berg, Anomalies in Dilute Metallic Solutions of Transition Elements, in: Prog. Low Temp. Phys., Vol. 4, Ed. C.J. Gorter (North-Holland, Amsterdam, 1964) p. 194.

[13] J. Kondo, Resistance Minimum in Dilute Magnetic Alloys, Prog. Theor. Phys. **32** (1964) 37.

[14] K.G. Wilson, The renormalization group: Critical phenomena and the Kondo problem, Rev. Mod. Phys. **47** (1975) 773.

[15] J. Kondo, The Physics of Dilute Magnetic Alloys, (Syokabo, Tokyo, 1983).

[16] N. Andrei, K. Furuya, and J. Lowenstein, Solution of the Kondo problem, Rev. Mod. Phys. **55** (1983) 331.

[17] J. Kondo, Two-Level Systems in Metals, in: Fermi Surface Effect, Eds. J. Kondo and A. Yoshimori, Springer Series in Solid-State Science Vol. **77** (Springer-Verlag, Berlin, 1988) p. 1.

[18] A.C. Hewson, The Kondo Problem to Heavy Fermions, Cambridge University Press, 1993.

[19] K. Yosida, Theory of Magnetism, Springer Series in Solid-State Science **122** (Springer-Verlag, Berlin, 1996).

[20] D.L. Cox and A. Zawadowski, Exotic Kondo Effects in Metals (Taylor and Francis, London, 1999).

[21] K. Yosida, Bound State Due to the *s-d* Exchange Interaction, Phys. Rev. **147** (1966) 223.

[22] A. Okiji, Bound State Due to the *s-d* Exchange Interaction–Effect of Higher Order Perturbations–, Prog. Theor. Phys. **36** (1966) 712.

[23] S.D. Silverstein and C.B. Duke, Greens's Function Derivation of the Low Equation for the Scattering Amplitude in Dilute Magnetic Alloy Systems, Phys. Rev. Lett. **18** (1967) 695-698.

[24] S.D. Silverstein and C.B. Duke, Theory of *s-d* Scattering in Dilute Magnetic Alloys. I. Perturbation Theory and the Derivation of the Low Equation, Phys. Rev. **161** (1967) 456-469.

[25] C.B. Duke and S.D. Silverstein, Theory of *s-d* Scattering in Dilute Magnetic Alloys. II. Derivation and Solution of Linear Vertex Equation, Phys. Rev. **161** (1967) 470-477.

[26] A.M. Tsvelick and P.B. Wiegmann, Exact results in the theory of magnetic alloys, Adv. Phys. **32** (1983) 453.

[27] A. Okiji, Bethe Ansatz Treatment of the Anderson Model for a Single Impurity, in Eds. J. Kondo and A. Yoshimori, Fermi Surface Effects, Springer Series in Solid-State Science Vol. 77 (Springer-Verlag, Berlin, 1988) p. 63.

[28] C. Zener, Interaction Between the *d* Shells in the Transition Metals, Phys. Rev. **81** (1951) 440.

[29] M.A. Ruderman and C. Kittel, Indirect Exchange Coupling of Nuclear Magnetic Moments by Conduction Electrons, Phys. Rev. **96** (1954) 99.

[30] K. Yosida, Magnetic Properties of Cu-Mn Alloys, Phys. Rev. **106** (1957) 893.

[31] T. Kasuya, A Theory of Metallic Ferro- and Antiferromagnetism on Zener's Model, Prog. Theor. Phys. **16** (1956) 45.

[32] T. Kasuya, *s-d* and *s-f* Interaction and Rare Earth Metals, in: Magnetism, Vol. IIB, Eds. G.T. Rado and H. Suhl (Academic Press, New York, 1966) p. 215.

[33] K. Yosida, Anomalous Electrical Resistivity and Magnetoresistance Due to an *s-d* Interaction in Cu-Mn Alloys, Phys. Rev. **107** (1957) 396.

[34] P.W. Anderson, Localized Magnetic States in Metals, Phys. Rev. **124** (1961) 41.

[35] K. Yosida and K. Yamada, Perturbation Expansion for the Anderson Model, Prog. Theor. Phys. Suppl. **46** (1970) 244;
K. Yamada, Perturbation Expansion for the Anderson Model. II, Prog. Theor. Phys. **53** (1975) 970;
K. Yosida and K. Yamada, Perturbation Expansion for the Anderson Model. III, Prog. Theor. Phys. **53** (1975) 1286;
K. Yamada, Perturbation Expansion for the Anderson Model. IV, Prog. Theor. Phys. **54** (1975) 316.

[36] T. Kasuya and T. Saso (Eds.), Theory of Heavy Fermions and Valence Fluctuations, Springer Series in Solid-State Science Vol. 62 (Springer-Verlag, Berlin, 1985).

[37] A. Sumiyama, Y. Oda, H. Nagano, Y. Ōnuki, K . Shibutani, and T. Komatsubara, Coherent Kondo State in a Dense Kondo Substance: $Ce_xLa_{1-x}Cu_6$, J. Phys. Soc. Jpn. **55** (1986) 1294.

[38] A. Yoshimori and H. Kasai, Theory of Dense Kondo System, J. Magn. Magn. Mater. **31-34** (1983) 475.

[39] A. Yoshimori and H. Kasai, Heavy Electrons in Alloys, Solid State Commun. **58** (1986) 259.

[40] S.D. Bader, Magnetism in low dimensionality, Surf. Sci. **500** (2001) in preparation.

[41] J.B. Goedkoop, Frontiers in nanomagnetism, Surf. Sci. **500** (2001) in preparation.

[42] J. Shen and J. Kirschner, Magnetism in artificially structure materials: The new frontier, Surf. Sci. **500** (2001) in preparation.

[43] M.F. Crommie, C.P. Lutz, and D.M. Eigler, Confinement of Electrons to Quantum Corral on a Metal Surface, Science **262** (1993) 218 .

[44] T. Kawasaka, H. Kasai, and A. Okiji, Adsorbate-induced charge density oscillations and many body effects in STM image, Phys. Lett. A **250** (1998) 403.

[45] T. Kawasaka, H. Kasai, W.A. Diño and A. Okiji, Spatial and spectroscopic profiles of the Kondo resonance for magnetic atoms on metal surfaces, J. Appl. Phys. **86** (1999) 6970.

[46] H. Kasai, W.A. Diño and A. Okiji, Behavior of a Magnetic Atom on a Metal Surface—Real Space Image of the Kondo Effect—, J. Electron Spectrosc. & Relat. Phenom. **109** (2000) 63..

[47] Donald M. Eigler, Private communication.

[48] H.C. Manoharan, C.P. Lutz, and D.M. Eigler, Quan-

tum mirages formed by coherent projection of electronic structure, Nature **403** (2000) 512.
[49] V. Madhavan, W. Chen, T. Jamneala, M.F. Crommie, and N.S. Wingreen, Tunneling into a Single Magnetic Atom: Spectroscopic Evidence of the Kondo resonance, Science **280** (1998) 567.
[50] J.T. Li, W.-D. Schneider, R. Berndt, and B. Delley, Kondo Scattering Observed at a Single Magnetic Impurity, Phys. Rev. Lett. **80** (1998) 2893.
[51] E.W. Plummer, L. Greene, and C. Yu, Surfaces: A Playground for physics with broken symmetry in reduced dimensionality, Surf. Sci. **500** (2001) in preparation.
[52] M. Crommie, Visualizing the quantum mechanical world with the STM, Surf. Sci. **500** (2001) in preparation.
[53] S. Hasegawa and F. Grey, Surface electron transport, From point-contact transistor to multi-tip STM, Surf. Sci. **500** (2001) in preparation.
[54] W. Ho, Chemistry one by one, Surf. Sci. **500** (2001) in preparation.
[55] H.-J. Güntherodt and R. Wiesendanger (Eds.), Scanning Tunneling Microscopy I, 2nd Edition, Springer Series in Surface Science Vol. 20, Springer-Verlag, Berlin, 1994.
[56] R. Wiesendanger and H.-J. Güntherodt (Eds.), Scanning Tunneling Microscopy II, 2nd Edition, Springer Series in Surface Science Vol. 28, Springer-Verlag, Berlin, 1995.
[57] C. Bai, Scanning Tunneling Microscopy and its Application, Springer Series in Surface Science Vol. 32, Springer-Verlag, Berlin, 1995.
[58] N.V. Smith, Phase analysis of image states and surfaces states associated with nearly-free-electron band gaps, Phys. Rev. **178** (1969) 1123.
[59] R. Paniago, R. Matzdorf, G. Meister, and A. Goldmann, Temperature dependence of Schockley-type surface energy bands on Cu(111), Ag(111) and Au(111), Surf. Sci. **336** (1995) 113.
[60] S.D. Kevan and R.H. Gaylord, High-resolution photoemission study of the electronic structure of the noble-metal (111) surfaces, Phys. Rev. **B36** (1987) 5809.
[61] C.J. Chen, Origin of Atomic Resolution on Metal Surfaces in Scanning Tunneling Microscopy, Phys. Rev. Lett. **65** (1990) 448.
[62] R.E. Watson, Iron Series Hartree-Fock Calculations. II, Phys. Rev. **119** (1960) 1933.
[63] M. Tsukada and N. Shima, Theory of Electronic Processes of Scanning Tunneling Microscopy, J. Phys. Soc. Jpn. **56** (1987) 2875.
[64] S. Crampin, Surface states as probes of buried impurities, J. Phys.: Condens. Matter **6** (1994) L613.
[65] W.A. Diño, K. Imoto, H. Kasai, and A. Okiji, Spatial and Spectroscopic Profiles of the Kondo Resonance for a Single Magnetic Atom on a Metal Surface under an External Magnetic Field, Jpn. J. Appl. Phys. **39** (2000) 4359.
[66] R. Wiesendanger, M. Bode, R. Drombowski, M. Getzlaff, M. Morgenstern, and C. Wittneven, Local Electronic Properties in the Presence of internal and External Magnetic Fields Studied by Variable-Temperature Scanning Tunneling Spectroscopy, Jpn. J. Appl. Phys. **37** (1998) 3769.
[67] K. Sueoka, K. Mukasa, and K. Hayakawa, Possibility of Observing Spin-Polarized Tunneling Current Using Scanning Tunneling Microscope with Optically Pumped GaAs, Jpn. J. Appl. Phys. **32** (1993) 2989.
[68] M. Mizuno, H. Kasai and A. Okiji, A model calculation for photo-stimulated desorption of molecules adsorbed on metal surface, Surf. Sci. **310** (1994) 273.
[69] H. Tsuchiura, H. Kasai and A. Okiji, A model calculation for photo-stimulated desorption, J. Phys. Soc. Jpn. **66** (1997) 2805.
[70] F. Abelés (Ed.), Optical Properties of Solids (North-Holland Publishing Company, Amsterdam, 1972).
[71] I.E. Tamm, Über eine mögliche Art der Elektronenbindung an Kristalloberflächen (On a possible type of electron binding at crystal surfaces), Phys. Z. Sowjet. **1** (1932) 733; Z. Physik **76** (1932) 849.
[72] W.B. Shockley, On the surface states associated with a periodic potential, Phys. Rev. **56** (1939) 317.
[73] P.M. Echenique and J.B. Pendry, Theory of Image States at Metal Surfaces, Prog. Surf. Sci. **32** (1989) 111-172.
[74] S.G. Davison and J.D. Levine, Surface States, in: Solid State Physics Vol. 525, Eds. H. Ehrenreich F. Seitz, and D. Turnbull (Academic Press, New York, New York, 1970) p. 1.
[75] R.M. Osgood, Jr. and X. Wang, Image state on single-crystal metal surfaces, in: Solid State Physics Vol. 51, Eds. H. Ehrenreich and F. Spaepen (Academic Press, San Diego, Chestnut Hill, 1998)]
[76] S.G. Davison and M. Stęślicka, Basic Theory of Surface States (Oxford Science Publications, New York, 1992).
[77] U. Höfer, I.L. Shumay, Ch. Reuß, U. Thomann, W. Wallauer and Th. Fauster, Time-resolved coherent photoelectron spectroscopy of quantized electronic states on metal surfaces, Science **277** (1997) 1480.
[78] T. Sakai, M. Sakaue, H. Kasai and A. Okiji, Theory of dynamics of electron wave packets in time-resolved two-photon photoemission via image states, Appl. Surf. Sci. **169-170** (2001) 57.
[79] A. Zangwill, Physics at Surfaces (Cambridge University Press, New York, 1988).
[80] M.C. Desjonquères and D. Spanjaard, Concepts in Surface Physics, 2nd edition (Springer-Verlag, Berlin, 1996).
[81] M. Sakaue, H. Kasai and A. Okiji, Theory of time-resolved two-photon photoemission from Cu(111): Effect of Coulomb interactions among electrons, Appl. Surf. Sci. **169-170** (2001) 68.
[82] M. Sakaue, H. Kasai and A. Okiji, Theory of time-resolved two-photon photoemission from a metal surface: The effect of Coulomb interactions between electrons, J. Phys. Soc. Jpn. **69** (2000) 160.
[83] T. Hertel, E. Knoesel, M. Wolf and G. Ertl, Ultrafast electron dynamics at Cu(111): Response of an electron gas to optical excitation, Phys. Rev. Lett. **76** (1996) 535.
[84] M. Wolf, E. Knoesel and T. Hertel, Ultrafast dynamics of electrons in image-potential states on clean and Xe-covered Cu(111), Phys. Rev. **B 54** (1996) R5295.
[85] A.A. Abrikosov, L.P. Gor'kov and I.E. Dzyaloshinskii, Quantum field theoretical methods in statistical physics (Pergamon Press, Oxford, New York, 1965) [translated to English by D.E. Brown, edited by D. ter Haar].
[86] L. Bartels, G. Meyer, K.-H. Rieder, D. Velic, E. Knoesel, A. Hotzel, M. Wolf and G. Ertl, Dynamics of electron-

induced manipulation of individual CO molecules on Cu(111), Phys. Rev. Lett. **80** (1998) 2004.

[87] M. Bauer, S. Pawlik and M. Aeschlimann, Decay dynamics of photoexcited alkali chemisorbates: Real-time investigations in the femtosecond regime, Phys. Rev. **B 60** (1999) 5016.

[88] S. Ogawa, H. Nagano and H. Petek, Optical decoherence and quantum beats in Cs/Cu(111), Surf. Sci. **427-428** (1999) 34.

[89] H. Petek, M. J. Weida, H. Nagano and S. Ogawa, Real-time observation of adsorbate atom motion above a metal surface, Science **288** (2000) 1402.

[90] M. Bauer, S. Pawlik and M. Aeschlimann, Femtosecond lifetime investigations of excited adsorbate states: atomic oxygen on Cu(111), Surf. Sci. 3**77-379** (1997) 350.

[91] A. Hotzel, K. Ishioka, E. Knoesel, M. Wolf and G. Ertl, Can we control lifetimes of electronic states at surfaces by adsorbate resonances?, Chem. Phys. Lett. **285** (1998) 271.

[92] M. Sakaue, H. Kasai and A. Okiji, The effect of interband excitations on time-resolved two-photon photoemission via a localized state at a metal surface, J. Phys. Soc. Jpn. **67** (1998) 2058.

[93] R. Hoffmann, A chemical and theoretical way to look at bonding on surfaces, Rev. Mod. Phys. **60** (1988) 601-628.

[94] R. Hoffmann, How Chemistry and Physics Meet in the Solid State, Angew. Chem. Int. Ed. Engl. **26**(1987)846-879.

[95] J.L. Whitten and H. Yang, Theory of chemisorption and reactions on metal surfaces, Surf. Sci. Rep. **218** (1996) 55-124.

[96] K. Hasegawa, H. Kasai, W.A. Diño and A. Okiji, Dynamics of STM-Induced CO Desorption from Cu(111), J. Phys. Soc. Jpn. **67** (1998) 4018; A microscopic theory of STM-induced CO desorption from Cu(111), Surf. Sci. **438** (1999) 283.

[97] M. Nishijima and F.M. Propst, Electron-Impact Desorption of Ions from Polycrystalline Tungsten, Phys. Rev. **B2** (1970) 2368.

[98] K. Fukutani, A. Peremans, K. Mase and Y. Murata, Photodesorption of NO from Pt(001) at $\lambda$ = 193, 248, and 352 nm, Phys. Rev. **B47** (1993) 4007; Photostimulated desorption of NO from a Pt(001) surface, Surf. Sci. **283** (1993) 158.

[99] H.J. Lee and W. Ho, Single Bond Formation and Characterization with a Scanning Tunneling Microscope, Science **286** (1999) 1719-1722.

[100] S.-W. Hla, L. Bartels, G. Meyer, and K.-H. Rieder, Inducing All Steps of a Chemical Reaction with the Scanning Tunneling Microscope Tip: Towards Single Molecule Engineering, Phys. Rev. Lett. **85** (2000) 2777-2780.

[101] K. Hasegawa, W.A. Diño, H. Kasai and A. Okiji, Dynamics of STM-induced acetylene rotation on Cu(100), Surf. Sci. **454-456** (2000) 1052-1057

[102] K. Hasegawa, H. Kasai, W.A. Diño and A. Okiji, Adsorbate dynamics induced by STM, Appl. Surf. Sci. **169-170** (2001) 25.

[103] B.C. Stipe, M.A. Rezaei and W. Ho, Coupling of Vibrational Excitation to the Rotational Motion of a Single Adsorbed Molecule, Phys. Rev. Lett. **81** (1998) 1263.

[104] K. Stokbro, B.Y.-K. Hu, C. Thirstrup, and X.C. Xie, First-principles theory of inelastic currents in a scanning tunneling microscope, Phys. Rev. **B58** (1998) 8038-8041.

[105] U. Kürpick and T.S. Rahman, Tip Induced Motion of Adatoms on Metal Surfaces, Phys. Rev. Lett. **83** (1999) 2765-2768.

[106] S. Corbel, J. Cerdá, and P. Sautet, Ab initio calculations of scanning tunneling microscopy images within a scattering formalism, Phys. Rev. **B60** (1999) 1989-1999.

[107] X. Bouju, C. Joachim, and C. Girard, Single-atom motion during a lateral STM manipulation, Phys. Rev. **B59** (1999) R7845-R7848.

[108] N. Mingo and K. Makoshi, Excitation of vibrational modes of adsorbates with the scanning tunneling microscope: many-orbital theory, Surf. Sci. **438** (1999) 261-270.

[109] N. Mingo and K. Makoshi, Calculation of the Inelastic Scanning Tunneling Image of Acetylene on Cu(100), Phys. Rev. Lett. **84** (2000) 3964.

[110] G. Binnig and H. Rohrer, Scanning Tunnelling Microscopy, Helv. Phys. Acta, **55** (1982) 726.

[111] G. Binnig, C.F. Quate, Atomic Force Microscope, Phys. Rev. Lett. **56** (1986) 930.

[112] L. Olesen, E. Lægsgaard, I. Stensgaard, F. Besenbacher, J. Schiøtz, P. Stoltze, K.W. Jacobsen, and J.K. Nørskov, Quantized Conductance in an Atom-Sized Point Contact, Phys. Rev. Lett. **72** (1994) 2251.

[113] F. Komori and K. Nakatsuji, Quantized conductance through atomic-sized iron contacts at 4.2K, J. Phys. Soc. Jpn. **68** (1999) 3786.

[114] H. Ohnishi, Y. Kondo and K. Takayanagi, Quantized conductance through individual rows of suspended gold atoms, Nature **395** (1998) 780.

[115] Y. Kondo and K. Takayanagi, Gold nanobridge stabilized by surface structure, Phys. Rev. Lett. **79** (1997) 3455.

[116] H. Kasai, K. Mitsutake, and A. Okiji, Effects of Confining Geometry on Ballistic Transport in Quantum Wires, J. Phys. Soc. Jpn. **60** (1991) 1679.

[117] H. Kasai, T. Kakuda, and A. Okij, Conductance quantization in a atom-sized contact between an STM-tip and a metal surface, Surf. Sci. **363**(1996) 428.

[118] Y. Kawahito, H. Kasai, H. Nakanishi and A. Okiji, Effects of Intra-site Coulomb Interaction on Quantized Conductance in a Quantum Wire between an STM-tip and a Metal Surface, Surf. Sci. **409** (1998) L709.

[119] Y. Kawahito, H. Kasai, H. Nakanishi and A. Okiji, Quantum Transport in an Atom-sized Bridge between a Metal Surface and a Tip of a Scanning Tunneling Microscope at Finite Temperatures, J. Appl. Phys. **85** (1999) 947.

[120] H. Nakanishi, H. Kasai and A. Okiji, Effects of the intra-site Coulomb interaction on electron transport in an atom bridge, Appl. Surf. Sci., in press.

[121] Y. Morigaki, H. Nakanishi, H. Kasai and A. Okiji, Quantized conductance in an atom-size bridge made from magnetic materials, J. Appl. Phys., in press.

[122] An interesting series of articles on how our work and society could be in the 21st century can be found online at http://www.time.com/time/reports/v21/home.html.

[123] C. Macilwain, Nanotech thinks big, Nature **405** (2000) 730.

[124] M.A. Reed and J.M. Tour, Computing with MOLECULES, Sci. Am. (June 2000) 69.

[125] W.A. Diño, H. Kasai, and A. Okiji, Orientational ef-

fects in dissociative adsorption/associative desorption dynamics of $H_2(D_2)$ on Cu and Pd, Prog. Surf. Sci. **63** (2000) 63.

[126] K. Sakamoto, H. Gouzu, K. Komiya, D. Kiga, S. Yokoyama, T. Yokomori, and M. Hagiya, Molecular Computation by DNA Hairpin Formation, Science **288** (2999) 1223.

[127] A. Cho, Hairpins Trigger an Automatic Solution, Science **288** (2999) 1152.

[128] S. Sun, C.B. Murray, D. Weller, L. Folks, and A. Moser, Monodisperse FePt Nanoparticles and Ferromagnetic FePt Nanocrystal Superlattices, Science **287** (2000) 1989.

[129] R.F. Service, Nanocrystal May Give Boost to Data Storage, Science **287** (2000) 1902.

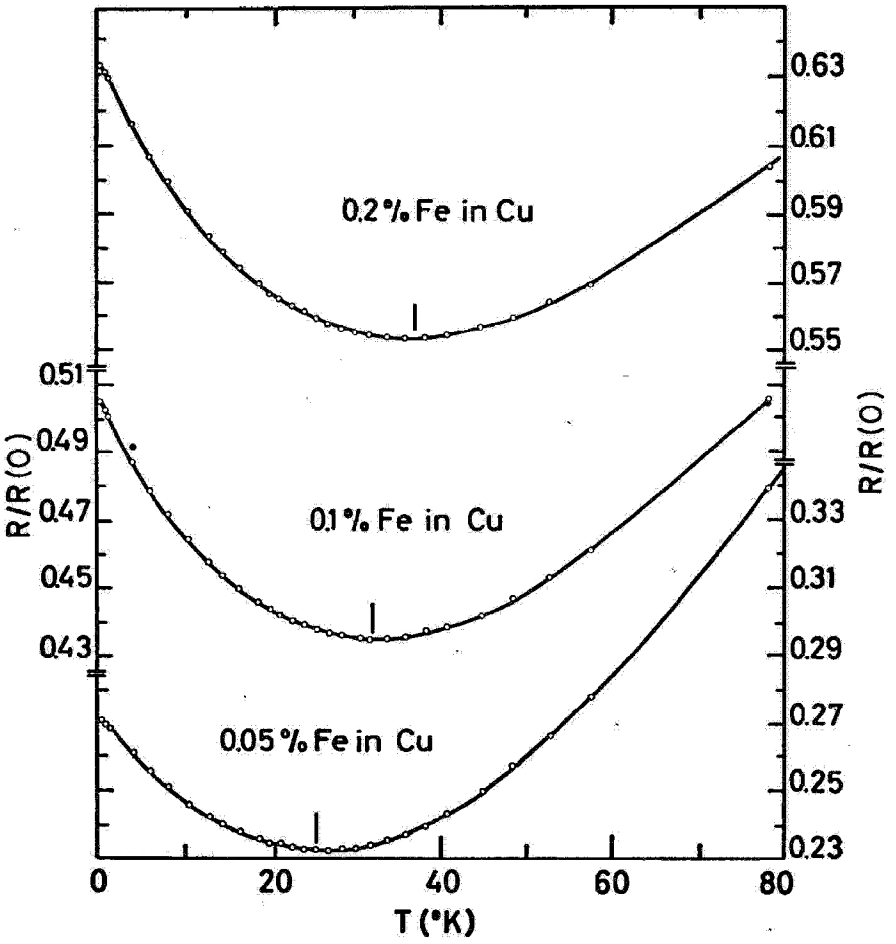


Fig. 1: The resistance minimum as a function of temperature for Cu with different concentrations of iron as impurity. $R(0)$ is the corresponding resistance at $T \approx 273$ K. The resistance minimum phenomenon is clearly evident. Note that the position of the minimum depends on the concentration of iron. From [11].

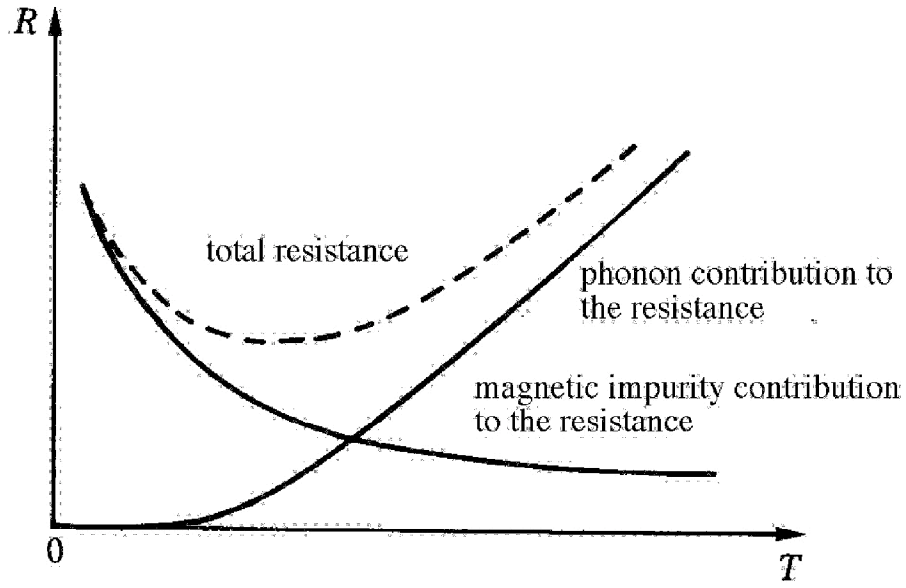


Fig. 2: Temperature $T$ dependence of the resistance $R$ associated with a low concentration of magnetic impurities in a metal. *Phonon contribution to the resistance*: Electric resistance is related to the amount of back scattering from defects and the vibrations of the atoms (phonons), which hinders the motion of the electrons through the crystal. The electric resistance of a pure metal usually drops as its temperature is lowered. This is because the vibrations of the atom (phonons) that impede the electrons gets smaller with decreasing temperature. However, the resistance saturates as the temperature is lowered below a certain critical temperature ($\approx$ 10 K) due to static defects in the material. The value of the low-temperature resistance depends on the number of defects in the material. Adding defects increases the value of this "saturation resistance" but the character of the temperature dependence remains the same. *Magnetic impurity contribution to the resistance*: The temperature dependence of the resistance changes dramatically when magnetic atoms, e.g., Fe, are added. Rather than saturating, the electric resistance increases as the temperature is lowered further, due to additional scattering of the electrons by the magnetic impurity through the interaction of their intrinsic angular momentum or "spin". The so-called Kondo temperature—roughly speaking the temperature at which the resistance starts to increase again—completely determines the low-temperature electronic properties of the material.

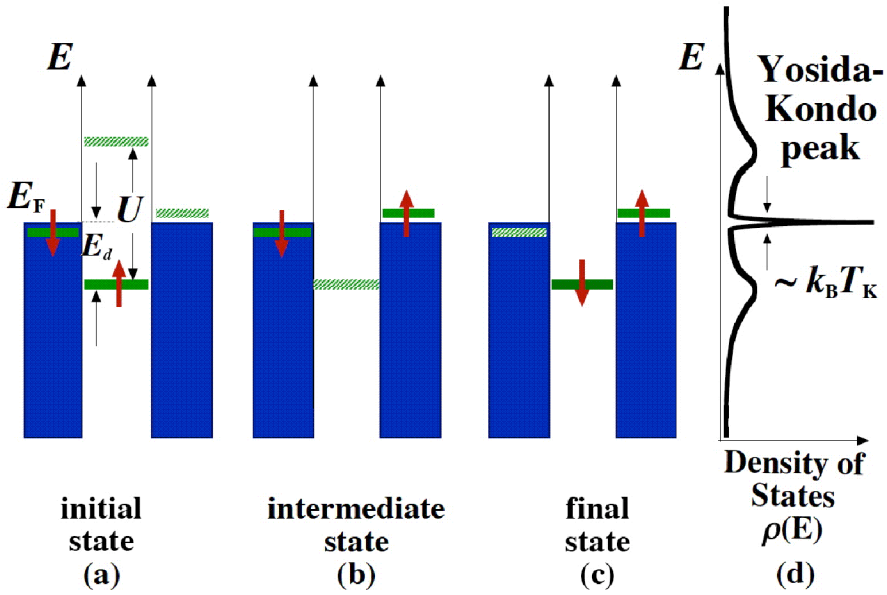


Fig. 3: Energy scheme of the Anderson model (the simplest model of a magnetic impurity, introduced by Anderson [34] in 1961) describing the energy structure of a magnetic impurity interacting with a sea of mobile (conduction) electrons—Fermi sea (blue). The Anderson model assumes that the impurity is described by a localized state (e.g., the $d$-orbital) occupied by a single electron with energy below the Fermi energy $E_{\mathrm{F}}$ of the metal. $E_d$ indicates the energy of the localized state of the magnetic impurity when it is occupied by a single electron of either spin $\uparrow$ or spin $\downarrow$ (red). Occupancy of the localized state by another electron of opposite spin results in an increase in the corresponding energy level by $U$, the Coulomb energy. Removing an electron from the localized state requires at least $|E_d|$. Although it is classically forbidden to take an electron from the localized impurity state without feeding energy into the system, in quantum mechanics, the Heisenberg uncertainty principle allows such a configuration to exist for a very short time—$\approx h/|E_d|$, where $h$ is Planck's constant. Thus, the spin $\uparrow$ electron initially occupying the the energy level $E_d$ (a), may tunnel out of the impurity site to briefly occupy a classically forbidden "intermediate state" (b) outside of the impurity. Within the time scale $h/|E_d|$, another electron must tunnel from the Fermi sea back towards the impurity (c). However, the spin of this electron may point in the opposite direction. Thus, the initial and final states of the impurity may have different spins. This spin "flipping" or spin exchange qualitatively changes the energy spectrum of the system (d). The Kondo effect is thus produced by a combination of such events taken together, and this results in the appearance of an extra resonance level/a new state (the singlet bound state) at the Fermi energy—- known as the Yosida-Kondo resonance (Yosida-Kondo peak) [21, 22] (d).

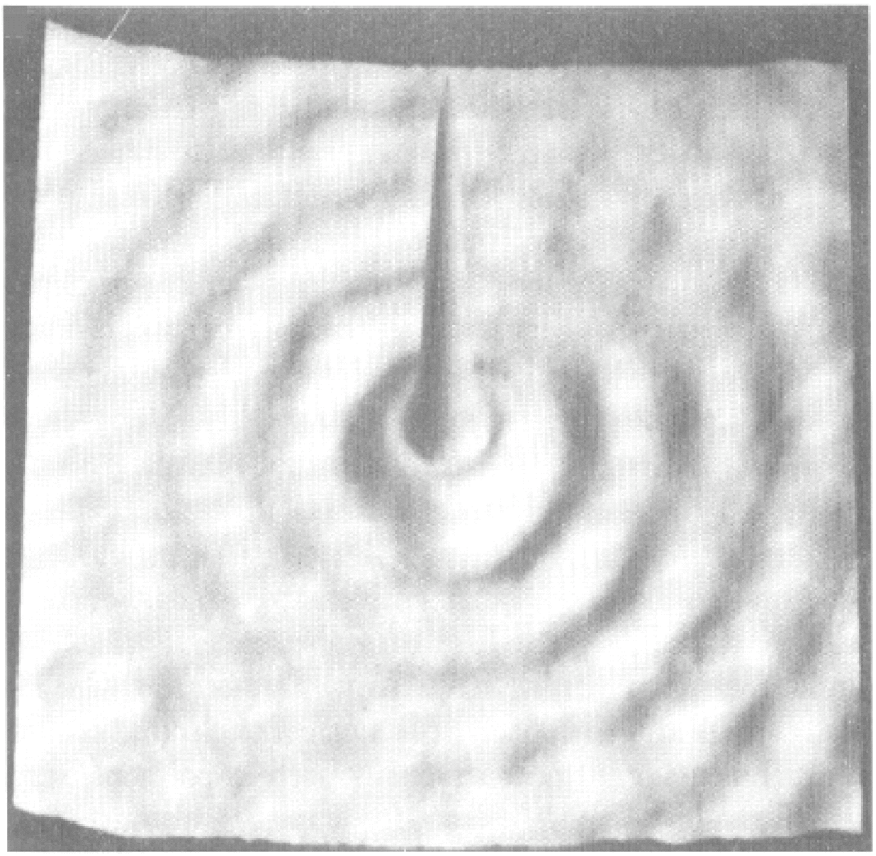

Fig. 4: (a) Constant current 130 Å×130 Å image of a single Fe adatom on a Cu(111) surface [acquired with a bias voltage (of the sample with respect to the STM tip) of $V = 0.02$ V, and current $I = 1.0$ nA]. The apparent height of the Fe adatom is 0.9 Å. The local density of states (LDOS) at the Fermi level $E_F$ surrounding the Fe adatom are marked by concentric rings (circular standing waves centered at the position of the Fe adatom), a result of the interaction/interference between the conduction electrons scattered by the Fe adatom. From [43].

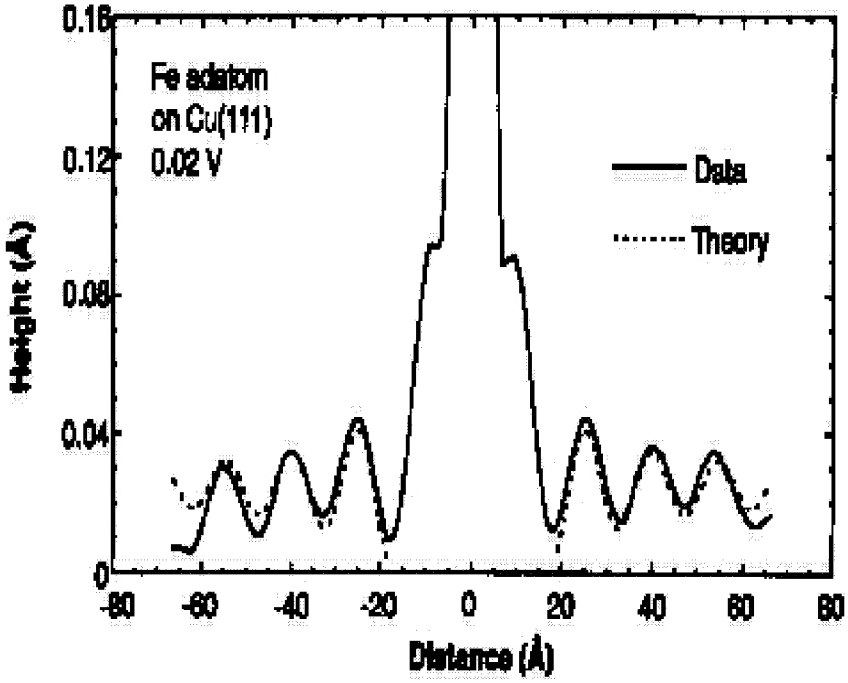


Fig. 4: (b) Solid line: cross sectional slice through the center of the Fe adatom image in (a). By modelling the Fe adatom as a cylindrically symmetric scattering potential, at low energies, the change in the LDOS at distances $r$ far from the Fe adatom ($r \geq \pm 20$ Å) can be approximated as $\propto \frac{1}{kr}\left[\cos^2(kr - \frac{\pi}{4} + \delta_0) - \cos^2(kr - \frac{\pi}{4})\right]$. $k = [2m^*E/\hbar^2]^{1/2}$. $m^*$ is the effective mass of a surface state electron ($0.38m_e$). $E$ is the energy measured from the surface-state band edge. Dashed line: obtained by fitting the experimental data (solid line) to the expression above, with $\delta_0 = -80^\circ \pm 5^\circ$ for the phase shift of the $l = 0$ scattered partial wave. From [43].

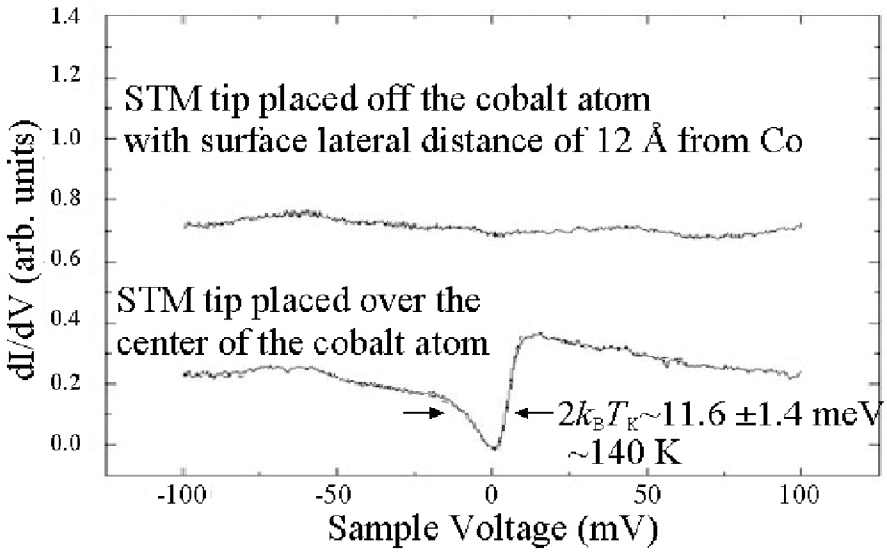


Fig. 5: A pair of $dI/dV$ spectra taken with the STM tip held over a single Co atom [acquired with a bias voltage (of the sample with respect to the STM tip) of $V = 0.1$ V, and current $I = 1.0$ nA] and over the nearby bare Au surface (a constant slope has been substracted from both curves, and they have been shifted vertically). The feature identified as a Yosida-Kondo resonance appears over the Co atom (the ratio of the amplitude of the resonance feature to the overall conductivity is 0.3). From [49].

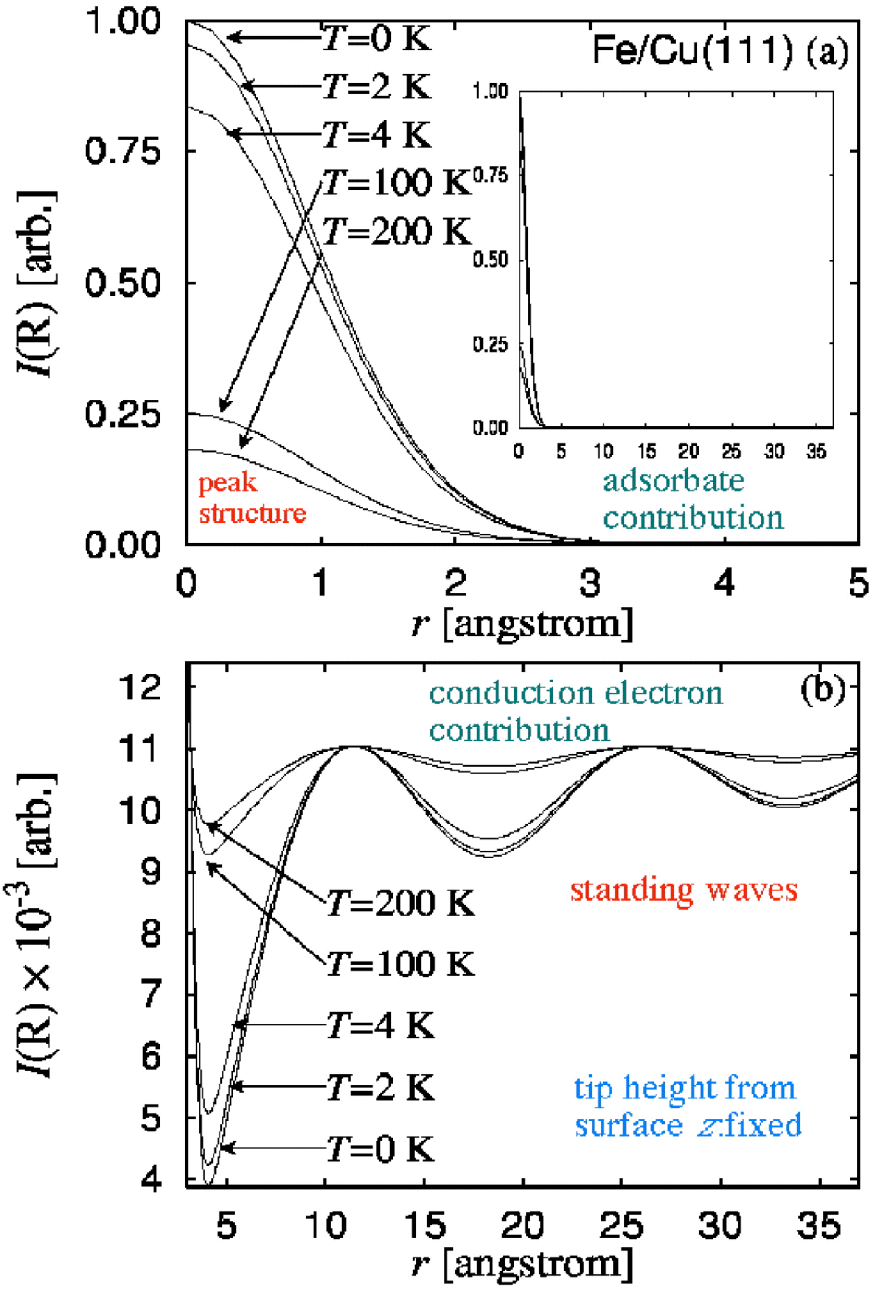


Fig. 6: Simulated tunnel current $I(\mathbf{R}) = I(x, y, z)$ [arbitrary units] as a function of the distance $r$[Å]=$\sqrt{x^2 + y^2}$ of the STM tip from Fe (which is located at $(x, y, z) = (0, 0, 0)$) and $T$ dependence (a) near Fe, (b) far from Fe. The STM tip is positioned at a distance $z = 4.0$Å from the surface. The wave number $k_z = i\lambda^{-1} = \sqrt{2m^*(\phi - E_F)}/\hbar$. The effective mass $m^* = 0.46m_e$ [58], where $m_e$ is the mass of a free electron. The workfunction $\phi = 4.94$ eV [59]. The Fermi energy $E_{\rm F} = 0.39$ eV, and the Fermi wave number $k_{\rm F} = 0.21$Å$^{-1}$ [60]. The decay constant $\lambda = 1.0$Å [61]. Here we assume that the localized orbital $\langle x, y, z|d\rangle$ is given by the $d_{3z^2-|\mathbf{R}|^2}$-orbital, which protrudes vertically from the surface [62]. $T_{\rm K} = 20$ K. Panel (a): results for $r$ =0-5 Å. Panel (b): results for $r$ =4-35 Å. From [44].

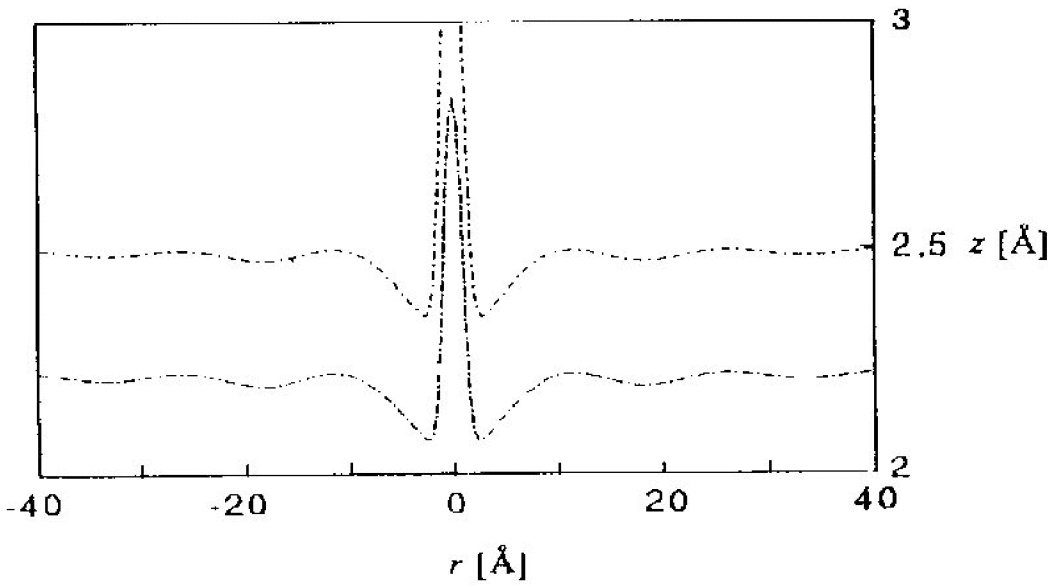


Fig. 7: Simulated STM tip height variation at constant current mode (corresponds to the spatial distribution of the density of states) and $T = 4$ K. The parameters are the same as those given in Fig. 6. We took $k_F = 0.21\text{Å}^{-1}$, based on results of photemission experiments on Cu(111) [60]. The slight difference in peak width as compared to experimental results can be attributed to our omission of the effects of the structure of the STM tip (*cf.*, Fig. 4 [43]). Inclusion of the effects of the STM tip structure [63] and the continuum of bulk-derived states [64] should give us the correct peak width. From [44].

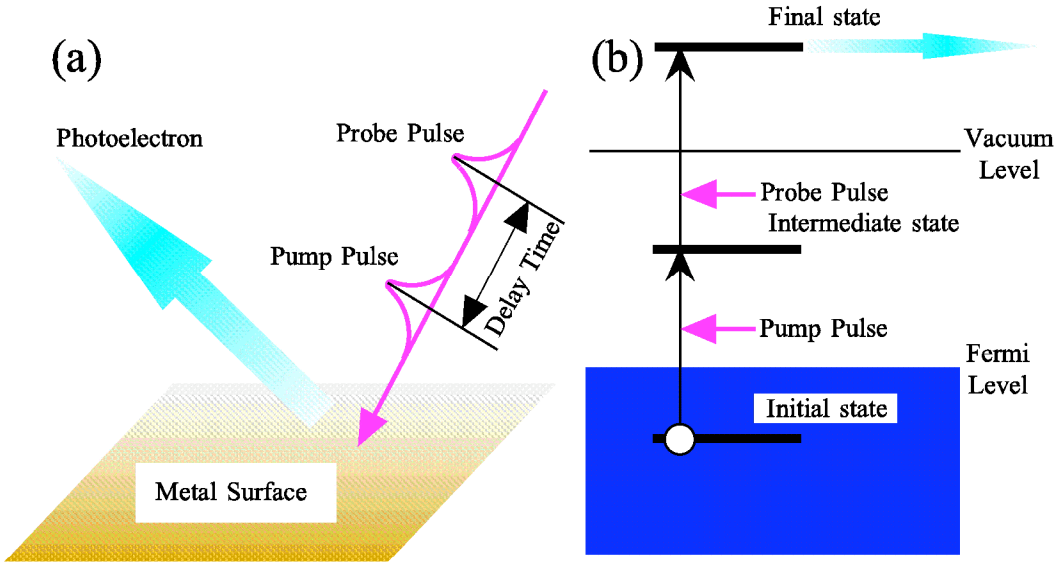


Fig. 8: (a) Schematic picture of TR2PPE spectroscopy. (b) Schematic diagram of the 2PPE process which may be described by a three level model. First an electron in an initial state is excited into an intermediate state by a pump photon and subsequently the electron is excited into a final state by a probe photon.

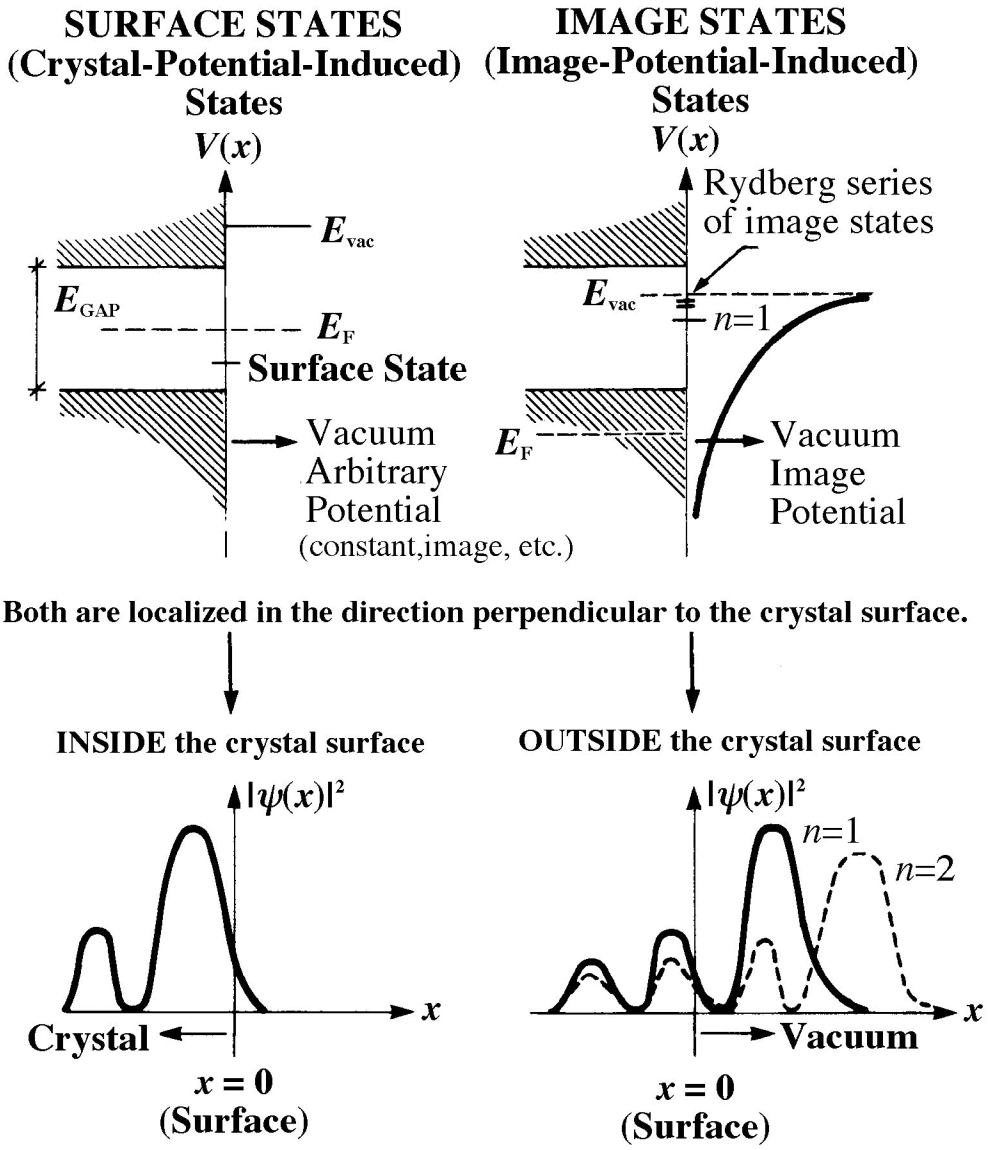


Fig. 9: Inside a perfectly periodic crystal, the electrons occupy Bloch states, i.e., the wave function of an electron moving in a crystal lattice, described by a periodic potential, has the form of a plane wave, modulated by a function which has the same periodicity as the periodic potential. Because of the breaking of the crystal three-dimensional symmetry, the surface of a solid introduces strong modifications into the electronic structure. These modifications come in the form of states appearing inside an electron energy band or between electron energy bands (inside electron energy band gaps). The wavefunctions (lower left panel) that represent these electrons decay strongly on both sides of the surface (bulk and vacuum). The electron states localized near the vicinity of solid surfaces are generally called surface states. Surface states located inside an electron energy band, called surface resonances, are sometimes distinguished from those located in band gaps, called proper surface states. The amplitude of the wavefunctions of the former decay exponentially into the bulk. The amplitude of the wavefunctions of the latter are still fairly localized in the surface region but can, however, leak into the bulk (persist throughout the crystal). It should be noted that the existence of surface states are influenced by the existence of impurities and defects at the surface, and they also exist near interfaces or point contact between two solids.

Historically, surface states are distinguished into two, depending on how surface states are modelled. Tamm states (after I.E. Tamm [71]) occur near band edges and are due to the difference in the potential at the surface and in the bulk. Shockley states (after W.B. Shockley [72]) occur within hybridizational band gaps far from band edges and require a multi-band model.

For completeness, we should also mention the image states (right panel) which are mainly located outside the surface. They refer to a Rydberg series (lower right panel) of states generated by the Coulombic tail of the image potential field associated with the electrostatic image force experienced by an electron outside a metal surface [73].

For more details, we refer the readers to the review articles by Davison and Levine [74], Echenique and Pendry [73], Osgood and Wang [75] and in the book by Davison and Stęślicka [76].

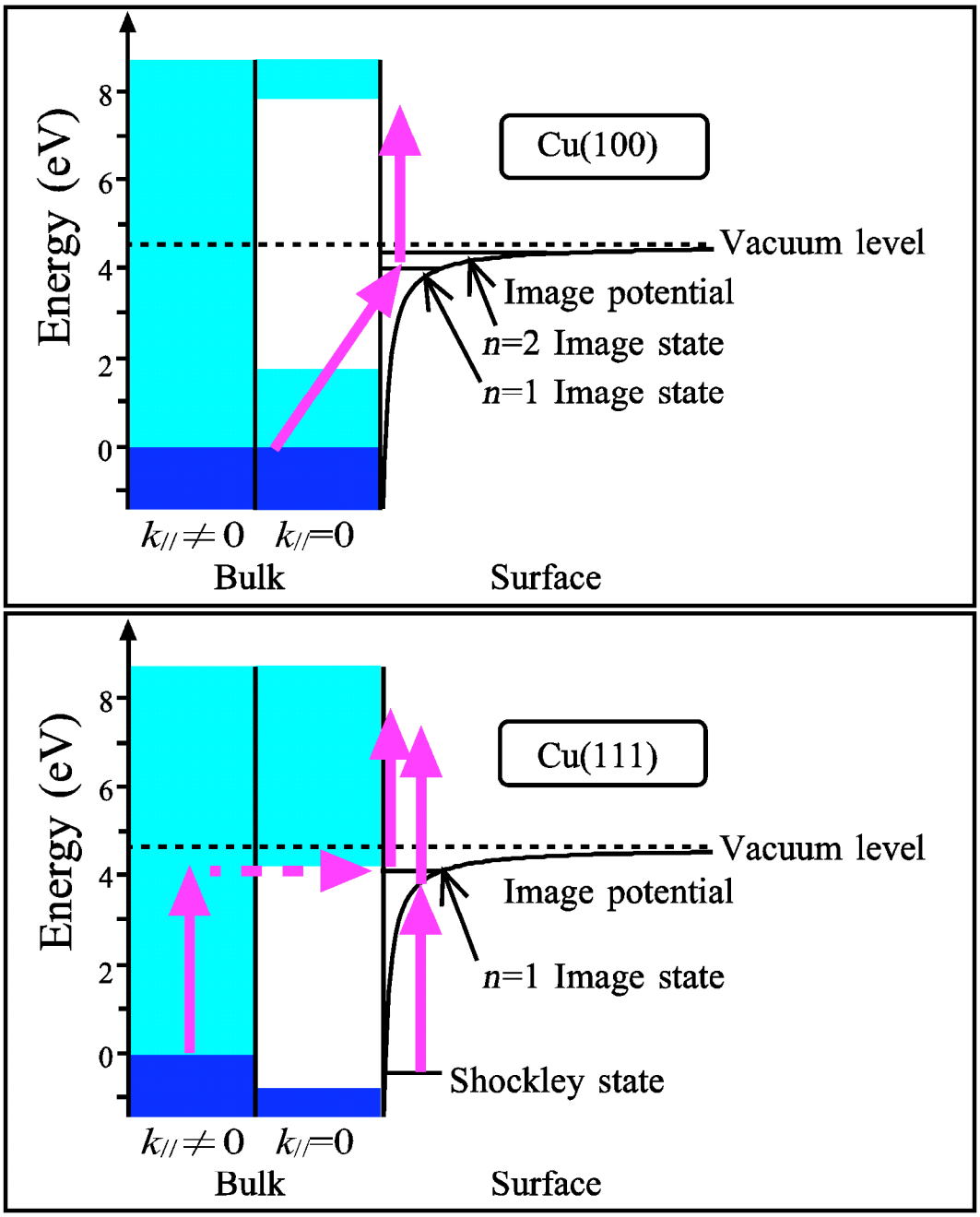


Fig. 10: Energy structure of the electron system of Cu(100) and Cu(111) and 2PPE processes (normal emission). $k_{//}$ gives the component of the electron wave vector parallel to the surface. Dark and light blue areas denote occupied and unoccupied bulk states. Horizontal lines in the right side denote surface localized states, *i.e.*, the image states and the Shockley state. In Cu(100), image states with quantum numbers $n \geq 3$ exists within the energy region between the energy level of the $n = 2$ image state and the vacuum level. Solid purple arrows denote excitation by UV and visible laser pulses, and broken arrow denotes electron transition into the image state by scattering due to Coulomb interactions between electrons. The energy level $E_n$ and wave function $\psi_n(z)$ of an image state with quantum number $n$ can be expressed approximately by simple formulae $E_n = E_{\rm vac} - 5\ {\rm eV} \times (n+a)^{-2}$ and $\psi_n(z) \propto \exp(-z/n^2) L_n(z)$. Here, $E_{\rm vac}$ gives the vacuum level, $z$ gives the distance of the electron from the surface, $a$ gives the quantum defect due to the difference between the effective potential for an electron in the vicinity of the surface and the classical image potential $-e^2/4z$, and $L_n(z)$ are Laguerre polynomials. From [75].

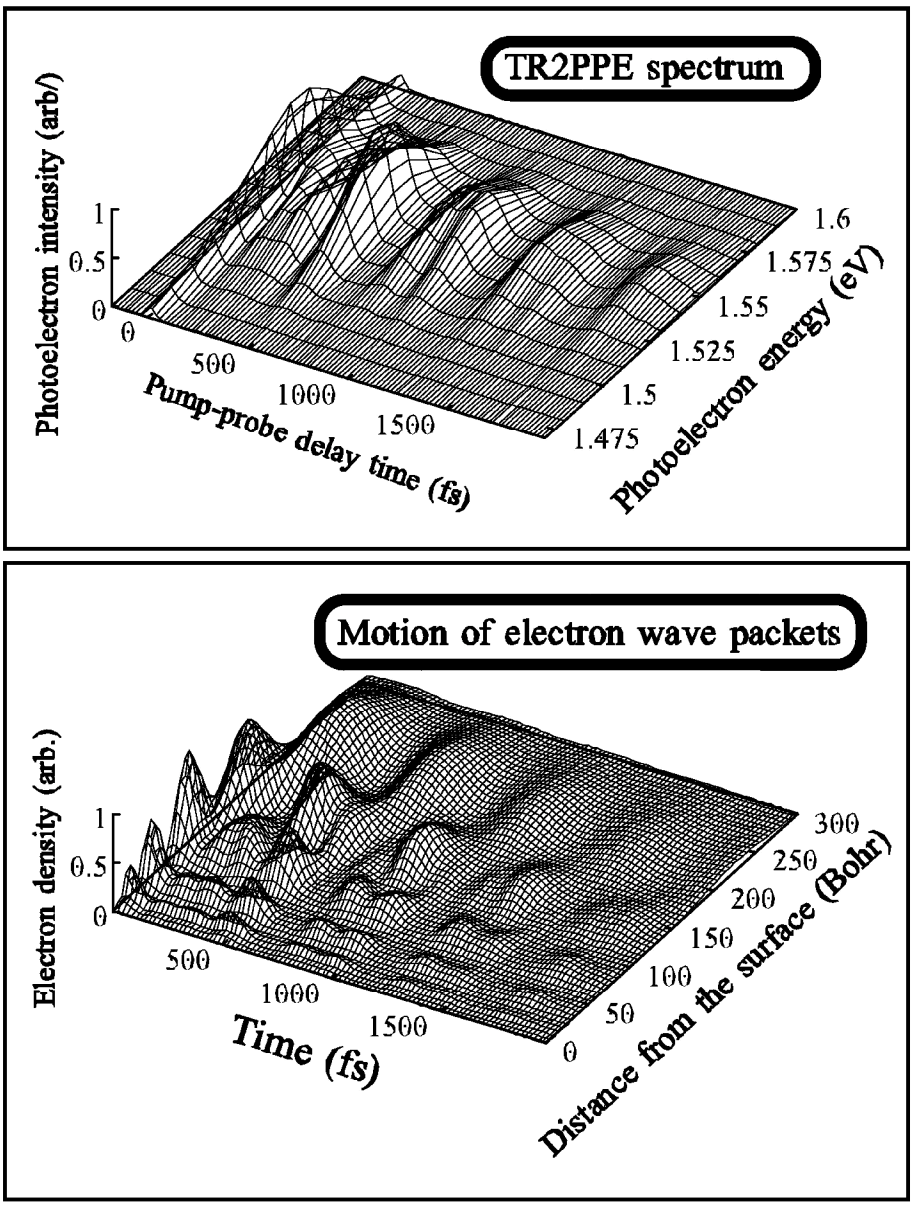


Fig. 11: Simulations [78] of the TR2PPE spectrum of Cu(100) (upper panel) and the electron density in the wave packets of the image states with quantum numbers 4, 5 and 6, $\sum_{n=4}^{6}\sum_{n'=4}^{6}\psi_{n'}^{*}(z)\langle n'|\rho(t)|n\rangle\psi_{n}(z)$, as a function of the time (the pump pulse intensity reaches a maximum at 0 fs) and the distance from the surface. Here, where $|n\rangle$ stands for the eigenvector of the image state with quantum number $n$ and $\rho(t)$ stands for the density matrix in the Schödinger representation. The origin of the energy is the vacuum level. The pump and probe photon energies are 4.7 and 1.57 eV and their durations are 95 fs. The TR2PPE spectrum shown in the upper panel provides information on the temporal change of the phase, which controls the motion of the wave packets shown in the lower panel. For example, the delay times when the photoelectron intensity in the upper panel reaches maxima ($t_{\rm d} \simeq 0$, 500 and 1500 fs) correspond to the times when the electron density in the vicinity of the surface in the lower panel reaches maxima.

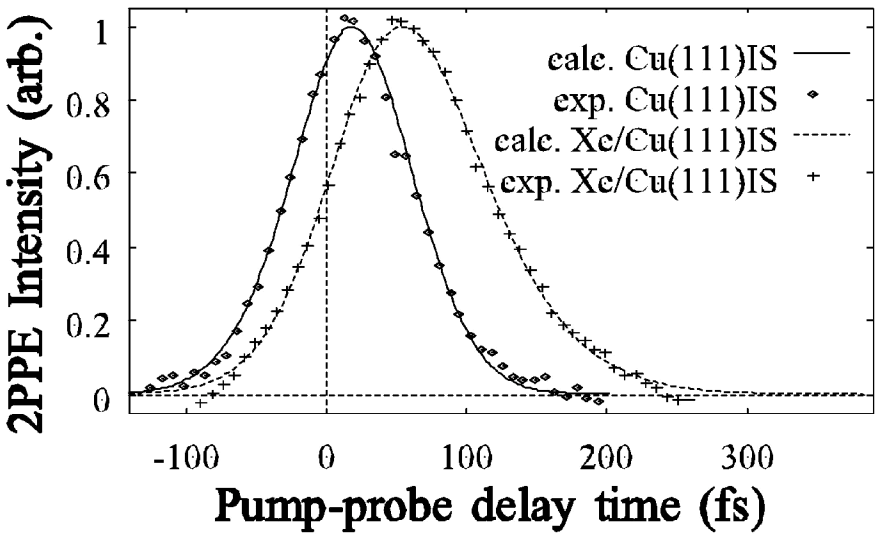


Fig. 12: Simulations [81] of the cross-correlation trace at the IS-peak in the TR2PPE spectrum of Cu(111). Solid and broken curves show the results for a lifetime of the electron in the image state $\tau_{10} = 7$ fs and a lifetime of the photoexcited electron or the hole $\tau_{\mu j} = 3$ fs, and those for $\tau_{10} = 30$ fs and $\tau_{\mu j} = 7$ fs, respectively. Here, the nonresonant transitions are neglected for simplicity. The pulse duration is obtained to be 59 fs by fitting the simulation correlation trace to the experimental data for the IS-peak [83, 84] considering the difference between the pump photon energy and excitation energies from the Shockley state to the image state. We see that the solid and dashed curves agree well with the experimental data for the clean Cu(111) surface (diamonds) [83] and those of the Xe/Cu(111) surface (crosses) [84].

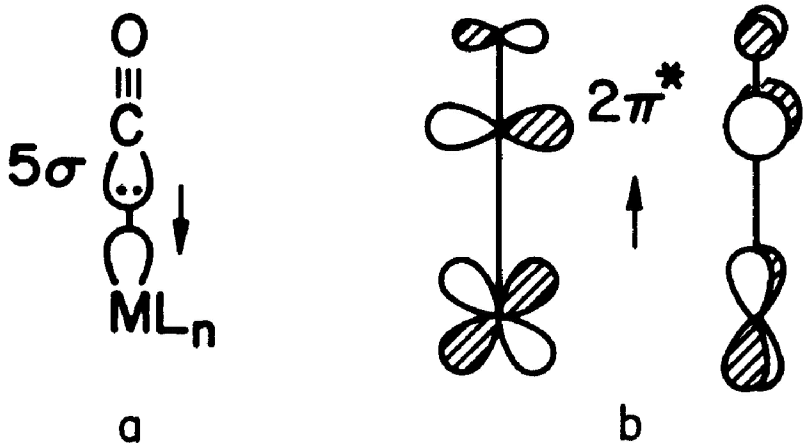


Fig. 13: Adsorption model of CO chemisorbed on a metal surface. A trace of the bonding in the chemisorbed CO reveals that the $2\pi^*$ interaction with the surface $d_\pi$ is responsible for a good part of the bonding. Panel (a) Forward donation from the carbonyl lone pair $5\sigma$ to some appropriate hybrid on a partner metal fragment. Panel (b) Back donation involving the $2\pi^*$ of CO and a $d_\pi$ orbital, $xz, yz$ of the metal. Shading corresponds to a positive phase of the wave function, and no shading corresponds to a negative phase of the wave function. Alternatively, shading may also mean a wave function with a positive sign, and no shading means the same wave function with a negative sign. From [93–95].

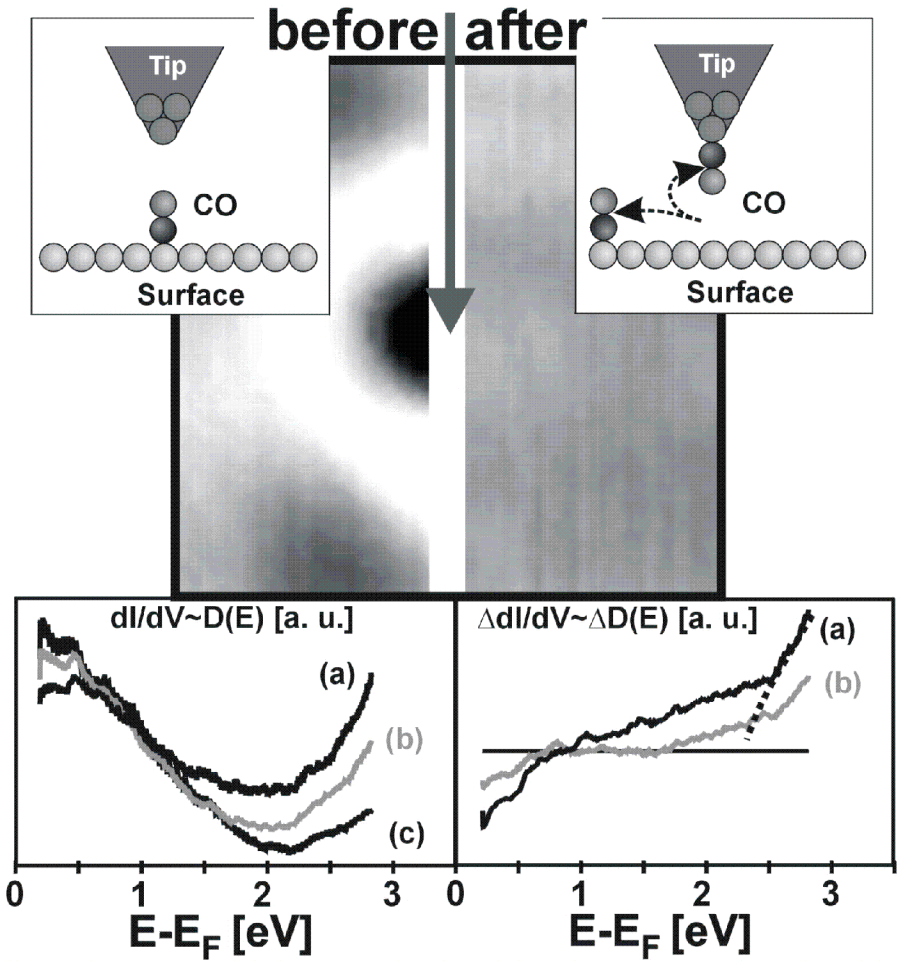


Fig. 14: Center: STM image of a single CO molecule on Cu(111) at 1.5 nA and 2 V. The left side of the 25 Å $\times$ 25 Å area, including the center of the CO molecule, is shown in the left panel. Throughout the experiment, the temperature is maintained at 15 K. The tip is subsequently positioned at the center of the image (top right sketch), and then the bias voltage is switched to 2.7 V for 3.8 seconds. During this time, an abrupt change in the simultaneously recorded tunneling current $I$ and local density of states of the sample $D(E) \approx dI/dV$ [in atomic units, measured as functions of the positive sample bias voltage $V \approx E - E_{\mathrm{F}}$] occurs, which can be interpreted as a transfer of the CO molecule away from its initial position to another adsorption site nearby (including the tip apex) (top left sketch), and as the scanning is resumed, the right side of the $25 \times 25$ Å area turns out dark, as shown in the right panel. Three $dI/dV$ spectra (bottom left diagram) are obtained by performing tunneling spectroscopy (a) at the center of the CO molecule, (c) at the edge of the image, and (b) in between–instead of inducing a transfer. The difference spectra $\Delta D(E) \approx \Delta dI/dV$ approximately reveal the CO-induced local density of states (bottom right diagram), which shows a rise above $\approx 1$ V followed by a steep increase starting at $\approx 2.4$ V (dashed line). From [86].

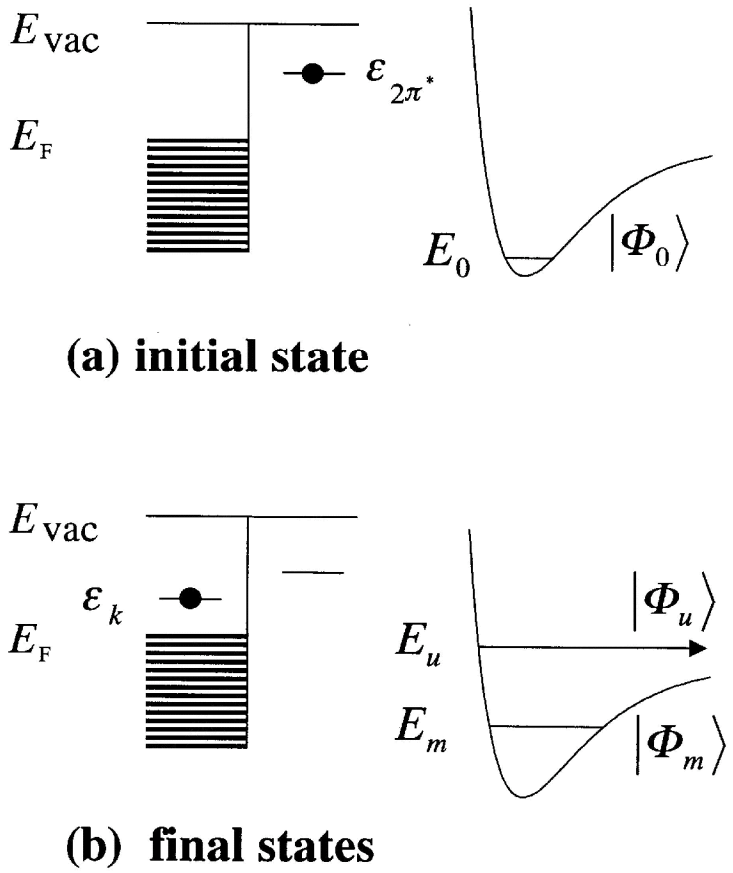


Fig. 15: Schematic energy diagram of the initial and final states of the CO/Cu(111) system. (a) The initial state configuration. The Fermi energy $E_{\rm F}$ is below the vacuum level $E_{\rm vac}$. The CO $2\pi^*$ orbital, with corresponding energy $E_{2\pi^*}$, is initially occupied by a single electron and the system is in the ground state CO-surface stretching vibration $|\Phi_0\rangle$. (b) The final states configuration. The single electron, initially occupying the CO $2\pi^*$ orbital, subsequently transfers/tunnels to the metal $|k\rangle$ orbital, with corresponding energy $\epsilon_k$, and the system is excited either into the $m$-th excited state of the CO-surface stretching vibration $|\Phi_m\rangle$ or an unbound state of the CO-surface stretching vibration $|\Phi_u\rangle$.